Light responses of melanopsin-expressing ganglion cells in the foetal mammalian retina

Jan Verweij[2, *], Shawnta Y. Chaney[2, *], Derek Bredl[2], Shruti Vemaraju[3], Gabriele M. König[6], Evi Kostenis[6], Richard A. Lang[3, 4,5], David R. Copenhagen[1*]

[1]Departments of Ophthalmology and Physiology, University of California, San Francisco, San Francisco, California Box 0444, 94158, USA

[2]Department of Ophthalmology, University of California, San Francisco, San Francisco, California 94143, USA

[3]The Visual Systems Group, Abrahamson Pediatric Eye Institute, Division of Pediatric Ophthalmology, Cincinnati Children's Hospital Medical Center, Cincinnati, OH 45229, USA

[4]Division of Developmental Biology, University of Cincinnati College of Medicine, Cincinnati, OH 45229, USA

[5]Department of Ophthalmology, University of Cincinnati College of Medicine, Cincinnati, OH 45229, USA

[6]Molecular, Cellular and Pharmacobiology Section, Institute of Pharmaceutical Biology, University of Bonn, 53115 Bonn, Germany

*Co-first authors

Author contributions

DRC and RAL provided project leadership. JV, SYC, DRC and DB designed and performed experiments and analysed data. DRC wrote the manuscript. JV, SYC, DB, SV and RAL critiqued the study and edited the manuscript. GMK and EK provided crucial reagents and advice.

Corresponding author:

David R. Copenhagen, Departments of Ophthalmology and Physiology, Box 0444, University of California, San Francisco, San Francisco, California 94158, USA. Tel: 415-502-7351 (Office), Fax: 415-476-6889. Email: cope@phy.ucsf.edu

Key points

- Melanopsin is a light-excitable photopigment expressed in a subset of ganglion cell neurons (mRGCs) in the retinas of many different species of vertebrates. In mature animals, light activation of mRGCs modulates many visual adaptive functions including pupil constriction, entrainment of circadian rhythms, mood and learning. In neonatal pups at ages prior to the developmental onset of visual signalling from rods and cones, melanopsin cells mediate photoaversive behaviour. In foetal pups, light activation of melanopsin cells accelerates maturation of the ocular vasculature. Here, we describe and physiologically characterize the light responses of melanopsin ganglion cells in the retinas of foetal pups.

- MRGCs in embryonic retinas respond to light at least four days prior to birth and exhibit responses to light of intensity as low as 3×10^{12} photons/cm^2/s.

- Phototransduction mechanisms include melanopsin activation of $G_{q/11}$ – G proteins, voltage-activated sodium currents, and voltage-gated L-type calcium currents.

- MRGCs are electrotonically coupled to other mRGCs in foetal retinas.

- We propose that melanopsin-expressing ganglion cells are excited by light while *in utero* and that this excitation relies, for the most part, on phototransduction pathways that have been described in postnatal retinas. Furthermore, we propose that foetal mRGCs have the requisite properties to modulate light-regulated maturation of the ocular vasculature and, perhaps, the development of visual pathways.

Abstract

Sensory stimulation plays a critical role in the maturation of sensory organs and systems. For example, when deprived of light before birth, foetal mouse pups *in utero* exhibit altered ocular vascular development. Normal vascular development depends on light excitation of melanopsin, a non-rod, non-cone photopigment that is expressed in a subset of ganglion cells (mRGCs) in the retina. However, there is no direct evidence that mRGCs in foetal eyes are light-responsive.

Very little is known about how light absorption leads to excitation in these foetal neurons. Using mRGC-specific expression of the calcium indicators GCaMP3 and GCaMP6, we report that foetal mouse mRGCs respond to light as early as 4 days before birth. Further, two distinct $G_{q/11}$-G protein family antagonists, FR9000359 and YM-254890, abolish these light responses. TTX, a blocker of voltage-activated sodium channels, reversibly represses light responses, and FPL6417 and L-cis-diltiazem, which modify L-type calcium channels, respectively increase and reduce light responses. Electrophysiological patch pipette recordings show that embryonic mRGCs respond to light of intensity as low as 2.9×10^{12} photons/cm^2/s. The present findings demonstrate a heretofore unproven but postulated light sensitivity in the retinas of foetal mice and identify the transduction pathways involved. Surprisingly, mRGCs do not function as completely independent photoreceptors but are electrotonically coupled with other mRGCs. Given that melanopsin is expressed in foetal human retinas, these findings support the idea that the eyes of foetal and early preterm infants are likely to exhibit functional photosensitivity. (241 words)

Introduction

Genetic programmes instruct the initial development of all organisms. Innate genetic programming also regulates the maturation of the eye and the visual system. However, light stimulation of maturing visual circuits also plays an important role in refining patterns of neural connectivity and establishing various types of functionality (Breedlove, 2017). Most previous studies have concentrated on the visually mediated refinement of visual centres at ages after rods and cones in the retina begin responding to light to generate visual signals. However, a unique class of intrinsically photosensitive melanopsin-expressing retinal ganglion cells (mRGCs) that can generate visual signals in the absence of input from rods and cones has been found in adult mammalian eyes (Berson et al., 2002; Do and Yau, 2010). In the eyes of foetal mice, markers of melanopsin expression can be observed 9 days before birth and 19 days before the emergence of visual signalling from rods and cones. In human eyes, markers of melanopsin expression appear at 8.5 weeks post-conception (31 weeks before birth) (Tarttelin et al., 2003). The presence of genetic and immunohistological markers for melanopsin raises the possibility that these mRGCs are intrinsically photosensitive and that light-mediated signalling may occur in embryonic eyes. Thus, ambient light from the pregnant mother's environment that penetrates to the eyes of foetuses might have the ability to control some aspects of foetal development. Indeed, mouse foetuses that are light-deprived during the final four days of gestation exhibit abnormal postnatal ocular vascular development (Rao et al.,

102 2013). Moreover, genetic deletion of melanopsin in foetal pups mimics the effects of light
103 deprivation (Rao et al., 2013). This finding suggests that ambient light passing through the
104 abdominal wall of the pregnant dam can activate melanopsin-expressing cells in foetal eyes and
105 trigger normal development of the ocular vasculature. A strong supporting argument in favour of
106 this hypothesis would be physiological evidence that mRGCs in the embryonic retina are light-
107 responsive. We report here that foetal mRGCs do respond to light.

108 Rods and cones in vertebrate retinas utilize opsin-based photopigments to capture light.
109 Rod and cone opsins couple to G-proteins belonging to the G_t (transducin) family to generate
110 photoresponses (Arshavsky et al., 2002). The photopigments in invertebrate photoreceptors,
111 unlike those in vertebrates, couple to non-transducin G-proteins. Rhodopsin in *Drosophila*
112 photoreceptors couples to G-proteins of the Gq family (Katz and Minke, 2009). Transduction of
113 light stimuli by melanopsin in postnatal mammalian retinas appears not to be coupled via G_t, but
114 the identity of the G-protein that mediates phototransduction remains controversial. Several
115 studies have demonstrated that mRGCs in postnatal mammals express one or more of four
116 different alpha subunits, *Gnaq*, *Gna11*, *Gna1* and *Gna15*, that are members of the $G_{q/11}$ gene
117 family (Chew et al., 2014; Graham et al., 2008; Hughes et al., 2015). Some studies have
118 suggested that melanopsin phototransduction is predominantly mediated by *Gnaq/11* coupling
119 (Hughes et al., 2015; Panda et al., 2005; Qiu et al., 2005). However, other reports concluded
120 that melanopsin functions independently of *Gnaq* and Gna*11* (Chew et al., 2014). In addition, in
121 expression systems, melanopsin can be coupled to $G_{i/o}$ (Bailes and Lucas, 2013) and to G_t
122 (Newman et al. 2003). Although the identification of melanopsin-G-protein coupling in postnatal
123 mice is somewhat controversial, a very recent study demonstrated that melanopsin-*Gnaq*
124 coupling is necessary and sufficient to trigger normal vascular development in the eyes of foetal
125 mice (Vemaraju et al. 2019). Direct measurement of light activity in mRGCs and
126 pharmacological intervention testing whether $G_{q/11}$ mediates the light responses of mRGCs in
127 foetal retinas and not merely ocular vascular development remains to be done.

128 We report here, using genetically encoded calcium indicator proteins expressed in
129 melanopsin cells, that embryonic mRGCs are light-responsive. We further show that
130 administration of the $G_{q/11}$ antagonists FR900359 and YM-254890 strongly attenuates these light
131 responses, supporting a role for melanopsin-mediated $G_{q/11}$-coupled signalling in
132 phototransduction. These findings convincingly establish that the melanopsin-expressing
133 ganglion cells in retinas of foetal mice as young as embryonic day 15.5 are light-responsive.
134 Given that the *Opn4* gene is expressed in human eyes at gestational week 9 (Tartellin et al.
135 2003), these results also raise the very interesting possibility that light sensitivity may be

136 conserved in the human foetus and that it may endow the foetal eye with previously
137 unrecognized photosensitivity.
138
139 **Methods**
140 **Animals**
141 The experiments were performed in accordance with the policy of The Journal of
142 Physiology and the rules and regulations set forth in the NIH Guidelines for
143 the Care and Use of Laboratory Animals. The Institutional Animal Care and Use Committee of
144 the University of California, San Francisco (Animal Welfare Assurance Number: A3400-01)
145 approved the experiments. The experiments also conformed to the Society for Neuroscience
146 Policy on the Use of Animals in Neuroscience Research. The mice were housed in an AALAC-
147 accredited pathogen-free animal facility at UCSF with ad libitum access to food and water.
148 The experiments were performed on mice of either sex with an age ranging from embryonic day
149 15.5 (E15.5) to postnatal day 2 (P2). The mice were housed on a 12-h light-dark cycle with
150 lights on at 7 AM and off at 7 PM. The following mouse strains were used to breed the
151 experimental animals in this study: *Opn4*^{cre} knock-in mice with Cre recombinase under the
152 control of the endogenous melanopsin promoter (Ecker et al., 2010); *Opn4*^{GFP} transgenic mice
153 with the green fluorescent protein gene driven by the melanopsin promoter (Schmidt et al.,
154 2008); Ai14 strain mice with the floxed tdTomato gene in the rosa26 locus (Madisen et al.,
155 2010); C57Bl/6J wild-type mice (Jackson Laboratory, Sacramento, CA); melanopsin knockout
156 mice (Panda et al., 2003); and finally Ai38(B6.Cg-*Gt(ROSA)26Sor*$^{tm38(CAG\text{-}GCaMP3)Hze}$/J) and AI96
157 (B6;129S6-Gt(ROSA)26Sor$^{tm96(CAG\text{-}GCaMP6s)Hze}$/J) strains with the floxed GCaMP3 and GCaMP6
158 genes, respectively, which encode two different calcium sensors, in the rosa26 locus (Jackson
159 Laboratory, Sacramento, CA; Zariwala et al., 2012). Genotyping of *Opn4*^{Cre} (Ecker et al., 2010),
160 *Opn4*$^{-}$ (Panda et al., 2002), *Ai14* (Madisen et al., 2010) and *Ai38* (Zariwala et al., 2012) mice
161 was performed as described in the referenced articles.
162
163 **Tissue preparation**
164 Pregnant females used in the calcium measurements were sacrificed by CO_2 inhalation followed
165 by cervical dislocation. For the electrophysiological experiments, pregnant females were
166 sacrificed by cervical dislocation. Following laparotomy, the uterine horns were removed and
167 transferred to cold ACSF (119 mM NaCl, 24 mM $NaHCO_3$, 1.25 mM NaH_2PO_4, 2.5 mM KCl, 2.5
168 mM $CaCl_2$, 1.5 mM $MgSO_4$, 10 mM glucose, 2 mM Na pyruvate, and 2 mM Na lactate) that had
169 been previously bubbled with carbogen (95%O_2/5% CO_2). The foetuses were dissected free of

170 their extra-embryonic membranes and decapitated, and the eyes were removed and placed in
171 carbogen-bubbled ACSF. For calcium imaging, the retina was freed from each eye under a
172 dissecting microscope, cut radially and teased, photoreceptor side down, onto a small piece of
173 plastic film; it was then flattened with a brush consisting of a single cat whisker while the plastic
174 film was dragged out of the solution on a microscope slide “boat ramp”. The plastic film was
175 lowered upside down onto a polylysine-coated (0.1 mg/mL) glass coverslip (Number 1, round,
176 12-mm diameter), and the plastic film was floated off the coverslip using a drop of ACSF. These
177 steps were performed under ambient room light at room temperature (RT). The coverslips were
178 kept in carbogen-bubbled ACSF (RT) in darkness until they were mounted in the recording
179 chamber. For each experiment, a coverslip was placed in the recording chamber (Warner
180 Instruments, Hamden, CT) and perfused with carbogen-bubbled ACSF at ~35°C flowing at 0.4
181 to 0.8 mL per minute. For patch-clamping, retinas were dissected and kept in carbogen-bubbled
182 ACSF. Immediately before each experiment, a radially cut retina was teased ganglion cell side
183 down onto a plastic film using a single cat whisker brush, dragged up the “boat” ramp, and
184 lowered photoreceptor side down onto a coated coverslip. After floating off the plastic film, the
185 coverslip was mounted in the preparation chamber.
186
187 **Patch clamping**
188 The perfused recording chamber was mounted on the stage of an upright Zeiss Axioskop FS
189 microscope equipped with infrared DIC optics and epifluorescence (470/40 excitation filter and
190 525/50 emission filter). An additional optical channel transmitted excitation from a high-wattage
191 480 nm LED (Sutter Instruments, Novato, CA). A factory-calibrated radiometer (Model S370,
192 UDT Instruments, San Diego, CA) was used to measure the incident irradiance at the retina.
193 Recordings were performed in ACSF heated to ~34°C using 3 stages of heating (a lab-designed
194 warming blanket near the supply reservoirs followed by a feedback-controlled inline heater and
195 a coverslip preparation chamber with a heated bottom (Cell MicroControls, Norfolk, VA) with
196 flow at approximately 1 mL/s. Patch clamp recordings were performed using an EPC-10
197 amplifier controlled by “PatchMaster” software (Heka Instruments, Holliston, MA). Glass pipettes
198 were formed from Sutter glass (BF150-110) on a Sutter P-97 electrode puller (Sutter
199 Instruments, Novato, CA). The pipettes were filled with 1 of 3 different patch pipette solutions.
200 The standard solution contained (in mM) 120 K gluconate, 5 NaCl, 4 KCl, 2 EGTA, 10 HEPES,
201 0.3 NaGTP, 4 MgATP, 7 phosphocreatine, and Tris-KOH (pH 7.3) and had an impedance of 4-6
202 MOhm. The Alexa pipette solution contained (in mM) 116 K gluconate, 2 EGTA, 10 HEPES, 0.3
203 NaGTP, 4 MgATP, 7 phosphocreatine tris, neurobiotin 12.4 (Vector Laboratories, Burlingame,

204 CA), Alexa 633 0.07% (Thermo Fisher Scientific, Waltham, MA) and was adjusted to pH 7.3
205 with KOH. The standard Lucifer yellow pipette solution contained 10% H_2O, 12.4 neurobiotin
206 and 0.2% Lucifer yellow CH (Sigma-Aldrich, St. Louis, MO). For amphotericin recordings, cell-
207 attached recording pipettes were filled with standard patch solution supplemented with freshly
208 mixed amphotericin B (0.1 mM, Sigma). Liquid junction potentials were measured (9 to 11 mV),
209 and the measured membrane potentials were corrected accordingly.
210 In the electrophysiological studies designed to record from identified light- responding mRGCs,
211 we used retinas harvested from *Opn4^{cre}::Ai96* embryos. To locate light-responsive ganglion
212 cells, we first recorded the fluorescent response of the entire field of ganglion cells to ~5s
213 epifluorescent stimulation (470/40 nm, 3 x 10^{17} - 3 x 10^{19} photons/cm^2/s excitation, 525/50 nm
214 emission). The locations of light-responsive fluorescent cells were marked on the screen
215 monitor. The same area of the retina was then viewed with infrared DIC optics, and the patch
216 pipettes were aligned with the cells showing light responses. Fluorescent and DIC images were
217 collected using a CCD camera (Hamamatsu Digital Camera C4742) and Micro-Manager
218 software (Open-image.com, San Francisco, CA).
219
220 **Intracellular calcium measurements**
221 *GCaMP calcium measurements:*
222 Epifluorescence from isolated retinas was imaged in an inverted Nikon (TE2000S) microscope
223 (20x S-Fluor objective, NA 0.75). A Lambda LS 175-watt stand-alone xenon arc lamp and power
224 supply (Sutter Instruments, Novato, CA) provided the light for stimulation. The incident light
225 passed through an FITC/TRITC filter set (51004v2 - peak excitation wavelength ~480 nm;
226 Chroma Technology Corp., Bellows Falls, VT). Stimulus-evoked epifluorescence was focussed
227 onto a CCD camera (either a Hamamatsu C4742; 1024*1280 pixels or a Hamamatsu Orca
228 Flash 4.0 LT; 2048x2048 pixels, Hamamatsu Corp., San Jose, CA). The field of view was ~ 430
229 µm x 340 µm (C4742) or ~ 650 µm x 650 µm (4.0 LT). Images were acquired using 4x4 binning
230 and had a resulting resolution of 512 x 512 pixels. Metafluor software (Molecular Devices, Inc.,
231 San Jose, CA) controlled stimulation and data acquisition. The excitation light simultaneously
232 activated GCaMP3 or GCaMP6 and stimulated melanopsin photopigment. Light stimuli were
233 presented at 2 Hz and 3 Hz. Stimulation/acquisition periods were 530 ms (2 Hz) and 330 ms (3
234 Hz). The photon flux at the retina was routinely 4 x 10^{17} photons/cm^2/s. Regions of interest
235 encircling the somas of GCaMP3-fluorescent ganglion cells were set manually on images
236 recorded from the best-focussed position. Fluorescence images from complete fields of view
237 were recorded continuously. The summed responses from all pixels within each separate ROI

238 were also viewed in real time and recorded to disc. Photobleaching of GCaMP3 was shown to
239 be minimal based on the very small decrease in fluorescence in GCaMP-expressing cells
240 lacking photopigment. Photoresponses could be repeatedly and reproducibly measured for
241 periods of up to 60 min.
242
243 *Calbryte-590 indicator dye*
244 *Exogenous calcium dye loading.* We used Calbryte-590™ AM dye (573 nm Ex/ 588 nm Em;
245 AAT Bioquest, Sunnyvale CA) to monitor intracellular calcium. This dye localizes to the
246 cytoplasm and is 10-fold brighter than Rhod-2 AM (Zhao et al. 2019). A 5 mM stock solution of
247 the dye in anhydrous DMSO was prepared just prior to use and diluted to a working solution of
248 20 μM by adding stock Calbryte-590™ AM solution to carbogen-bubbled ACSF containing
249 Pluronic F-127 (0.04% f.c.). Isolated retinas were incubated in the ACSF/Calbryte-590™
250 solution for 2 hours in the dark with continuous carbogen circulation; they were then rinsed with
251 fresh ACSF, mounted ganglion cell side down on a polylysine-coated (0.1 mg/mL) glass
252 coverslip and placed in a heated (37°C) perfusion chamber. Calcium imaging was performed on
253 the same optical rig used for the GCaMP experiments.

254 **Immunohistochemical labelling**
255 For GCaMP3/melanopsin immunohistochemistry, the eye was removed, the cornea was
256 perforated with a razor blade, and the entire eye was immediately immersed in 4% (w/v)
257 paraformaldehyde (PFA) in PBS. In some experiments, the anterior part of the eye, including
258 the cornea and lens, was first carefully removed before immersing the entire posterior eyecup in
259 fixative. The eye was fixed in PFA in 0.1 M PBS for 30–90 min at RT. The eye was then stored
260 overnight in 25% sucrose, 0.01% sodium azide in 0.1 M PBS at 4°C. The following day, the
261 eyes were embedded in OCT and frozen on dry ice. Twenty-micron sections of the retina were
262 cut perpendicular to the vitreal surface with a cryostat, mounted on Super-Frost Plus slides
263 (Fisher Scientific, Pittsburgh, PA), and stored frozen at −20°C until immunostaining. ToPro3
264 (Life Technologies, Waltham, MA, Cat. # T3605) staining was used to mark nuclei. UF008
265 (1:500, Advanced Targeting Systems, San Diego, CA) and goat anti-GFP (1:500, Novus
266 Biologicals, Littleton, CO) were used to label melanopsin and GCaMP3/GCaMP6, respectively.
267
268 **Drugs**

269 FR900359 was isolated from the dried leaves of *Ardisia crenata* according to a
270 previously published procedure (Schrage et al., 2015). YM-254890, tetrodotoxin, FPL65176 and
271 L-cis-diltiazem were purchased from Wako Chemicals (Osaka, Japan), Calbiochem
272 [MilliporeSigma] (Temecula, CA), Tocris Bio-Techne Corporation (Minneapolis, MN) and
273 MilliporeSigma (Temecula, CA), respectively.

274 **Results**
275
276 **Cells in foetal mouse retinas are light-responsive as detected by the fluorogenic calcium**
277 **indicator dye Calbryte-590™**.
278 Melanopsin ganglion cells in foetal mouse pups differentiate before birth (Tartellin et al.
279 2003). In postnatal mouse retinas, mRGCs and perhaps other types of cells coupled to mRGCs
280 are light-responsive, as demonstrated by stimulus-evoked increases in intracellular calcium
281 levels (Sekaran et al. 2005). Photosensitive cells have not been reported in the retinas of
282 embryonic mice or any other embryonic mammal. To determine whether such photosensitive
283 cells exist, we searched for light responses by monitoring the activity of cells in embryonic
284 mouse retinas after exogenously bulk-loading the retinas with the calcium-sensitive dye
285 Calbryte-590™ AM (Zhao et al. 2019). After harvesting, the flat-mounted retinas were
286 fluorescently imaged, immersed in Calbryte-590™ AM, mounted in a perfusion chamber, bathed
287 with ACSF at 35°C, and stimulated with light of wavelength 480 nm (see Methods). Figure 1A
288 shows an example of a Calbright-590™-loaded 340 µm x 430-µm region cropped from the full
289 image (650 nm x 650 nm). This retina was harvested from an E17.5 mouse pup. The image was
290 captured from the video recording at the onset of the light stimulus. Figure 1B shows an image
291 of the same retina captured 2.5 s after stimulus onset. Figure 1C, which is a difference image
292 (Fig. 1B minus Fig. 1A), accentuates the light-evoked increase in fluorescence that reflects the
293 increase in intracellular calcium in the cells. The time courses of calcium increases in four of the
294 cells, marked with circular regions of interest, are plotted in Fig. 1D. Peak changes in calcium
295 centred approximately 2 s after the onset of the light. In total, we recorded Calbryte-590™
296 images in 2 to 3 animals taken from 3 different litters at age E17.5 and 2 litters at E18.5. We
297 commonly detected more than 100 light-dependent calcium responses in each 430 mm x 340
298 mm region of the retina. Analysis of 4 of the brighter cells is shown in Figure 1.

299 Non-OPN4 opsins such as encephalopsin (OPN3) and neuropsin (OPN5) are expressed
300 in the retina. Cells that express these opsins might also exhibit light-evoked Calbyte-590™
301 signals (Buhr et al., 2015, Kumbalasiri and Provencio, 2005). In mouse eyes, markers for
302 neuropsin and encephalopsin appear after 10.5 days of gestation (Tarttellin et al. 2003). We
303 tested foetal retinas from melanopsin knockout mice (*Opn4*^{cre} homozygotes) and never
304 observed a light-evoked increase in Calbright-590™ fluorescence in these retinas. These
305 findings support the interpretation that the light-evoked calcium increases we observed in foetal
306 retinas were evoked in OPN4 cells and that no detectable calcium elevations were observed in
307 OPN3- or OPN5-expressing cells. It is noteworthy that light stimulation of OPN5 cells has been
308 shown to modulate ocular dopamine levels in early postnatal mice (Nyugen et al. 2019).
309 In summary, the data presented here provide strong evidence that a subpopulation of
310 cells within the foetal retina exhibits light-dependent calcium responses. However, we cannot
311 rule out the possibility that the observed light responses reflect light-evoked activity from non-
312 mRGCs as well as from mRGCs. For example, Calbryte-590™ AM dyes (and likely other AM
313 indicator dyes) can indiscriminately load into cells of various types, including astrocytes
314 (Tirschbirek et al. 2015). Thus, neurons or glial cells coupled to mRGCs could also exhibit light-
315 evoked activation (Sekaran 2003; Reifler 2017). To address these ambiguities, we designed an
316 experimental approach to selectively restrict the expression of calcium indicators to mRGCs.
317
318
319 Figure 1 near here
320
321
322 **Melanopsin ganglion cells in foetal retinas are light-responsive as shown by the**
323 **responses of the calcium indicator GCaMP3 expressed exclusively in mRGCs.**
324 We first asked whether the genetically encoded calcium indicator GCaMP3 is selectively
325 expressed in mRGCs of mouse retina. We utilized the Ai38 mouse strain in which GCaMP3 is
326 conditionally expressed. In the progeny of *Opn4*$^{cre/+}$::*Ai38* mice, an allele that encodes the
327 EGFP-based Ca^{2+} reporter GCaMP3 is transcribed in cells that express Cre recombinase
328 (Zariwala et al. 2014). Because the *Opn4* gene is expressed relatively early in gestation, we
329 reasoned that we could expect to observe conditional GCaMP3 expression well before birth and
330 that it would be possible to detect light-evoked calcium signals that were restricted to
331 melanopsin-expressing cells. Figure 2 A-C shows flat-mounted retinas in which melanopsin
332 immunofluorescence co-localizes with EGFP immunoreactivity. This confirms that GCaMP3 is

333 expressed in mRGCs. Of note, we also observed a population of GCaMP3-positive cells that
334 showed little, if any, melanopsin immunoreactivity. The melanopsin-immunoreactive cells we did
335 observe are likely to be predominantly mRGCs of the M1 subtype, which express high levels of
336 melanopsin (Ecker et al. 2010). The other GCaMP3-EGFP-labelled cells may correspond to
337 other mRGC subtypes that express melanopsin Cre but are known to express lower levels of
338 melanopsin. In radial cryosections, an EGFP signal was evident in the inner plexiform layer and
339 was strong in neurons with RGC morphology (Fig. 2D). These anatomical findings demonstrate
340 that GCaMP3 is indeed localized to mRGCs. It should be noted that the images shown in Figure
341 1A-D were obtained from postnatal mice. Although CGaMP3 was well expressed in embryonic
342 retinas, melanopsin antibody staining of prenatal retinas was not consistently detected.
343 Therefore, based on the co-localization of antibody staining, it cannot be persuasively argued
344 that the GCaMP3 cells in the foetal retinas co-expressed functional melanopsin protein.
345 However, given that we were able to record light-evoked calcium increases in most of the
346 embryonic GCaMP3-positive cells of the inner retina, there is little doubt that melanopsin protein
347 was expressed in these foetal RGCs. The light sensitivity of mRGC-GCaMP3 embryonic
348 neurons in retinae was next characterized.
349 To search for light responses in foetal eyes, we mechanically isolated retinas from foetal
350 pups, placed them in a perfusion chamber and stimulated them with light at 480 nm, the
351 wavelength of light to which the melanopsin photopigment is most sensitive. Light stimulation
352 resulted in $[Ca^{2+}]_i$ increases in GCaMP3-expressing neurons localized across the ganglion cell
353 layer of the isolated retinas. Single-frame images of GCaMP3-filled RGCs show fluorescence in
354 the retina of an E16.5 mouse before the onset of the stimulus (Fig. 2E) and during a light
355 response (Fig. 2F). The complete time courses of changes in $[Ca^{2+}]_i$ in the 4 encircled cells (Fig.
356 2E) are shown in Fig. 2G. The black line in Fig. 2G shows the averaged response of all 79 cells
357 recorded in this experiment. These records reveal that the time-to-peak following light onset
358 ranged from 1.5 s to 4 s. The response kinetics were comparable to those reported in previous
359 studies of postnatal mRGCs (Ecker et al. 2010, Hartwick et al. 2008, Sekaran et al. 2005). We
360 also measured and plotted a cumulative histogram of peak response amplitudes (Fig. 2H). The
361 responses of the individual cells (Fig. 2G) were taken from the 20th, 40th, 60th and 80th percentile
362 groups (Fig. 2H). We discerned no correlation between peak amplitude and time course and no
363 obvious partitioning of responses, suggesting that the temporal differences noted in different
364 mRGC subtypes in postnatal mice are not evident at this age (Tu et al., 2005).
365 In total, we examined 1 to 4 littermates from 12 different embryonic litters. In
366 *Opn4$^{cre/+}$::Ai38* foetal pups, we found light-responsive cells in 6 of 6 litters. In *Opn4$^{cre/+}$::Ai96*

367 foetal pups, we observed light responses in 16 of 16 litters. Using our standard irradiance
368 stimulus (3.8 x 10^{16} photons/cm^2/s), we recorded up to 90 responsive cells in 430 µm x 340 µm
369 regions of the retinas. The fact that as many as 90% of the GCaMP3-positive cells exhibited
370 light responses argues against the possibility that artefactual Cre expression may have occurred
371 in non-melanopsin-producing cells (Delwig et al., 2016; Ecker et al., 2010). We were able to find
372 detectable $[Ca^{2+}]_i$ elevations with stimulus irradiances as low as 3 x 10^{16} photons/cm^2/s. At
373 stimulus irradiances below that level, the signal-to-noise ratios were too low for reliable
374 detection.
375 No light responses were observed in control experiments performed in melanopsin
376 knockout retinas. *Opn4*$^{cre/+}$*::Ai38* mice crossed with *Opn4*$^{cre/cre}$ mice produce some
377 *Opn4*$^{cre/cre}$*::Ai38* pups. The mRGCs in these pups express GCaMP3 but not melanopsin. We
378 found no light-responsive cells in these foetal pups (Fig. 2G, inset). The experiments with
379 knockout retinas also serve to rule out the possibility that the light-evoked increase in GCaMP3
380 fluorescence in melanopsin-expressing cells is an artefact unrelated to melanopsin-mediated
381 calcium influx. Additionally, the recordings in knockout cells reveal that bleaching of GCaMP3 is
382 minimal under our experimental conditions. Specifically, the fluorescence amplitude 10 seconds
383 after light onset was 94 ± 3% of the initial amplitude (Fig. 2G, inset).
384 In summary, these results convincingly demonstrate that mRGCs in foetal mouse retinas are
385 responsive to light. In addition, the Calbryte590™ measurements in OPN4 knockout mice
386 suggest that any photo-responses generated by other opsins, such as OPN3 and OPN5, were
387 below the limit of detection.
388
389
390 Figure 2 near here
391
392

393 **Antagonists of the $G_{q/11}$ G-protein family attenuate mRGC light responses in foetal retina.**

394 Light-activated opsins in invertebrate eyes signal via coupling to members of the $G_{q/11}$
395 family of G-proteins (Katz B & Minke B., 2009). Similarly, light-activated melanopsin in mRGCs
396 has been postulated to signal via a comparable $G_{q/11}$ pathway (Panda S et al., 2005; Hughes et
397 al., 2015; Graham DM et al., 2008; Jiang et al., 2018). However, a recent study reported that
398 deletion of $G_{q/11}$ G-proteins does not abolish light responses in postnatal mRGCs (Chew et al.,
399 2014). We tested whether $G_{q/11}$ signalling plays an essential role in embryonic mRGC light

400 responses. To do this, we examined the effects of two different cell- permeable antagonists,
401 FR900359 (Schrage et al., 2015) and YM-254890 (Kawasaki et al., 2003; Nishimura et al.,
402 2010), on light responses. These two compounds inhibit activation of the Gnaq, Gna11 and
403 Gna14 alpha subunits of $G_{q/11}$-G proteins. For these experiments, we used *Ai96* mice that
404 express the calcium indicator GCaMP6. GCaMP6 has superior sensitivity and a better
405 signal/noise ratio than GCaMP3 (Chen et al., 2013). The methods of breeding and fluorescence
406 recording were otherwise identical to those used with the *Ai38* animals in the previous
407 experiments. Recordings were made in *Opn4*$^{cre/+}$*::Ai96* retinas harvested from E15.5 and E16.5
408 foetal pups. The retinas were placed in control medium (ACSF), and light responses were
409 recorded from mRGCs before and after the addition of YM-254890 at 200 nM or FR900359 at 1
410 μM. Figure 3A shows an example of a recording from one retina; the light responses, quantified
411 as the increase in light-induced fluorescence, dF/F, were stable over a 40-min period in ACSF
412 but were progressively attenuated during the 30-min period following the addition of YM-
413 254890. Four representative light responses on an expanded time scale are shown (Fig. 3B).
414 We found no evidence of reversibility following washout. Poor reversibility has been reported
415 previously (Yasui et al., 2008). The time courses of the mean light responses from multiple
416 mRGCs in each retina are shown in Fig. 3C and D. Both YM-254890 (E15.5 retina, 32 mRGCs)
417 and FR900359 (E16.5 retina, 43 mRGCs) severely attenuated light responses after 30 min. To
418 rule out the possibility that the inhibitors merely killed the mRGCs or quenched the
419 fluorescence, we applied high potassium (50 mM) at the end of the inhibitor infusion. Figure 3D
420 shows an example in which potassium substitution was able to induce a dF/F larger than that
421 originally induced by light.
422 Prolonged incubation in 200 nM YM-254890 reduced the average dF/F of the light
423 responses to 7% ± 11% of that of the control responses (n=93). Prolonged incubation in 1 μM
424 FR900359 reduced the average dF/F of the light responses to 4% ± 18% that of the control
425 responses (n=219). Comparing light responses from individual cells prior to and during drug
426 application, we found highly significant drug effects across the ensemble of responsive cells.
427 According to the Wilcoxon Signed Rank Sum Test for paired data, the two-tailed $P = 2.01948e^{-28}$
428 for YM and was even smaller for FR.
429 The use of two independent Gnaq/11/14 inhibitors diminishes the possibility that off-
430 target effects of either FR900359 or YM-254890 are responsible for the observed suppression
431 of light responsiveness. These results implicate $G_{q/11}$ signalling in the generation of light
432 responses in embryonic mRGCs. One caveat is that the averaged data shown in Figure 3 may
433 not reflect the presence of subpopulations of mRGCs that might utilize non-$G_{q/11}$ pathways.

434
435
436 Figure 3 near here
437
438
439

440 **No subgroups of $G_{q/11}$-independent mRGCs in embryonic retinas are detected in**
441 **population data.**

442 Jiang et al. (2018) reported that in adult mice most classes of mRGCs employ a $G_{q/11}$
443 cascade for transduction. However, they also reported that M4- type mRGCs utilize a second
444 alternative transduction cascade involving a cyclic nucleotide as the second messenger and
445 HCN channels. Jiang et al. (2018) reported that this pathway very likely does not use $G_{q/11}$
446 family members or TRP6/7 ion channels. In support of this conclusion, they showed that M4
447 mRGCs responded to light normally in cells devoid of *Gnaq*, *Gna11* and Gna14 as generated in
448 Gnaqfl/fl;Gna11$^{-/-}$;Gna14$^{-/-}$mouse eyes transfected with Cre-GFP via adeno-associated virus
449 serotype 2 (AAV2-CMV-Cre-GFP).

450 We hypothesized that if a group of mRGCs in foetal retinas also does not use $G_{q/11}$
451 signalling, then a subpopulation of GCaMP6-expressing mRGCs should be resistant to the
452 action of YM and FR. Figure 4, below, shows cumulative data from 93 mRGCS tested in YM-
453 254890 and 219 mRGCs tested in FR900359. Our data indicate that only approximately 1% of
454 the cells might be resistant to these drugs. Thus, our experiments provide no supportive
455 evidence for the existence of a detectable subpopulation of foetal mRGCs that utilize a non-G
456 $_{q/11}$ transduction pathway.
457
458 Figure 4 near here
459
460
461
462
463
464
465

466 **TTX-sensitive sodium currents amplify mRGC light responses in embryonic retinas.**

467 Based on electrophysiological recording and calcium measurements from neonatal
468 mRGCs harvested from rat retinas, Hartwick et al. (2007) proposed a transduction pathway in

469 which melanopsin-driven G-protein activation leads to the opening of cationic TRPC6/7
470 channels. The resulting inward cation flux subsequently depolarizes the membrane, leading to
471 activation of TTX-sensitive sodium action potentials and then to activation of L-type calcium
472 channels, which, in turn, increases calcium ion influx. We sought to determine whether TTX-
473 sensitive sodium and L-type calcium currents support light responses in embryonic mRGCs.
474 The likelihood of finding a role for TTX-sensitive currents in embryonic mRGC responses is
475 enhanced by previous work demonstrating that a majority (78%) of randomly selected RGCs in
476 E15 mouse retinas expressed TTX-sensitive sodium currents (Rorig and Grantyn, 1994).
477 We found that TTX (1 μM) reversibly diminished the average light response amplitudes
478 of virtually all the foetal GCaMP6-expressing mRGCs we tested. Figure 5 shows the responses
479 recorded from 177 cells in 4 E16.5 retinas. Each solid data point (blue) denotes the light
480 response amplitude in TTX (ordinate) as a function of the amplitude in control ACSF prior to
481 TTX (abscissa). The open circles show the responses of the same cells after washout of TTX.
482 We found that TTX effectively reduced the light responses to below the detectable threshold in
483 21% of the cells ($dF/F < 0.05$). The aggregate differences between responses in TTX versus
484 washout are highly significant (Wilcoxon Signed Rank Test for paired data, two-tailed $P = 1.01e^{-}$
485 ^{46}). Of note, these data show that while TTX reversibly diminished the light responses in virtually
486 all of the tested mRGCs, the effects of TTX varied across the sample of cells. This variability is
487 at odds with Hartwick et al. (2007), who reported that TTX abolished responses nearly
488 completely in all mRGCs (n = 8). The observed difference in the efficacy of TTX could reflect
489 our sampling of a larger population of mRGCs. Alternatively, these findings might reflect cell-
490 specific differences in the maturation of INa(V) channels during embryonic and postnatal
491 development. Nonetheless, we conclude that these TTX-sensitive channels do serve to amplify
492 the light-evoked responses in a plurality of embryonic mRGCs.
493
494 Figure 5 near here
495

496 **Modifiers of L-type voltage-gated calcium channels modulate the light responses of**
497 **mRGCs in E16.5 mouse retinas.**

498 Previously, Hartwick et al. (2007) showed that L-type voltage-gated calcium channels
499 account for most of the calcium influx that occurs following light stimulation of enzymatically
500 isolated postnatal rat mRGCs. While there are no reports of L-type calcium channels specifically
501 in mRGCs of embryonic retinas, earlier studies suggested that L-type calcium channels are
502 expressed in unspecified, randomly selected RGCs in E15 mouse retinas (Rorig and Grantyn,

503 1994). Consistent with this finding, expression of two L-type channel subunits, Cacna1a and
504 Cacna1b, in the eyes of E15.5 mouse pups has been reported (Allen Brain Atlas, Cacna1a – RP
505 090930_03_A09 – sagittal; Cacna1b - RP_090707_03_G11 - sagittal). We tested
506 pharmacologically for evidence that L-type calcium channels contribute to the light responses of
507 GCaMP3-expressing mRGCs. In one set of experiments, we found that L-*cis*-diltiazem, a
508 blocker of L-type calcium channels (Catterall et al., 2005), significantly diminished light
509 responses in embryonic retinas (n=3). Figure 6 shows the results obtained from 31 cells that
510 were recorded simultaneously in one retina. Panel A shows examples of reversible L-cis-
511 diltiazem-induced suppression of light responses in 5 mRGCs. Panel B plots the responses
512 from all mRGCs in which the light response peak amplitude returned to a value between 80 and
513 120% of that observed under control conditions upon washout. The blue dots plot the responses
514 in L-cis-diltiazem, and the black dots plot the amplitude of the responses following washout. The
515 five circled data points correspond to the light responses shown in Fig 6A. The effect of L-cis-
516 diltiazem is highly significant according to the Wilcoxon Signed Rank Test for paired data (two-
517 tailed $P = 9.31e^{-10}$).
518
519 Figure 6 near here
520
521
522
523
524 In a complementary set of experiments, we found that FPL64176, an activator of L-type
525 calcium channels (Zheng et al., 1990), increased light-evoked dF/Fs in embryonic mRGCs. In
526 previous studies, FPL64176 was shown to enhance the activity of retinal L-type calcium
527 channels. Specifically, FPL64176 enhanced L-type calcium-mediated evoked release of the
528 neurotransmitter glycine from amacrine cells (Bieda & Copenhagen, 2004). In addition,
529 FPL64176 potentiated spontaneous waves of activity that occur in neonatal retinas (Singer et
530 al., 2001). Figure 7 plots the peak light-evoked fluorescent responses observed before and
531 during exposure of explanted retinas to FPL64176 (2 μM). The data include the responses from
532 147 GCaMP3-expressing mRGCs from 2 different E16.5 retinas. The responses observed
533 during treatment with FPL64167 are plotted against the responses observed under control
534 conditions. On average, the df/F values in FPL64176 were 0.22 ± 0.02 (SEM) larger than dF/F
535 in control. The blue line shows the best linear regression fit to the FPL64176 data (y = 1.51x).
536 The black line shows the values that would be expected if FPL64176 had no effect on the light

537 responses. The Wilcoxon Rank Sum Test for paired data yielded a two-tailed P value of $1.172e^{-}$
538 ^{32}. Together, the L-cis-diltiazem and FPL-64176 findings strongly support a role for L-type
539 calcium channels in the generation of the light responses, similar to the transduction role
540 proposed by Hartwick et al. (2007) for postnatal mRGCs.
541
542 Figure 7 near here
543
544 **Voltage-activated sodium currents exist ubiquitously in mRGCs from at least E16.5**
545 Having found that the INa (V) antagonist TTX reduces and sometimes completely
546 abolishes light responses in embryonic mRGCs, we sought to characterize these sodium
547 currents electrophysiologically. Using patch pipettes, we recorded from mRGCs genetically
548 marked with either GCaMP6, tdTomato or EGFP derived from *Opn4*^{cre}::Ai96, *Opn4*^{cre}::Ai14, or
549 *Opn4*^{EGFP} mouse strains, respectively. Patch pipettes were directed towards the fluorescently
550 marked cells in isolated flat-mounted retinas. In the GCaMP-labelled retinas (*Opn4*^{cre}*::Ai96*), we
551 recorded from only those RGCs that displayed light-evoked calcium responses as reported by
552 GCaMP6. An example of a voltage clamp recording from an mRGC in E18.5 retina is shown in
553 Fig. 8. Panels A-C show current responses to a series of sequentially larger 10 mV voltage
554 steps initiated at –70 mV (see Panel E). Brief, transient inward currents began to occur at – 40
555 mV and became faster with successive depolarizing pulses (Panel A). Perfusion with TTX (1
556 μM) reversibly blocked the inward currents (Panels B and C). The evoked TTX-sensitive
557 currents (Panel D) were isolated by subtracting the response in Panel B from Panel A. The
558 voltage dependence of the TTX-sensitive currents is plotted in Panel F. The peak current
559 amplitude (black dots) exhibited a sharp onset at -40 mV, reached a maximum at -30 mV and
560 then declined with further depolarizing steps. The kinetics and voltage dependency of the TTX
561 currents shown here resemble those of the canonical INa(V) currents observed in excitable
562 muscle and nerve cells across multiple phyla (Johnston & Wu, 1995).
563
564 **The mean amplitudes of INa (V) currents increase substantially from E16.5 to P1-3.**
565 INa (V) currents were detected in virtually all of the mRGCs recorded in 10 E16.5, 35
566 E18.5 and 7 P1-3 retinas. The peak INa (V) currents (not all data were analysed and included)
567 are plotted in Fig. 8 (Panel G). The mean peak currents in the aforementioned groups of retinas
568 were 320, 674 and 1986 pA, respectively. Comparable developmentally linked increases in the
569 amplitude of INa(V) currents have been reported in random samplings of RGCs in mouse and
570 rat retinas (Rorig and Grantyn, 1994; Schmid and Guenther, 1996). Our findings confirm that

571 functional voltage-dependent sodium channels are expressed in mRGCs as early as E16.5 and
572 further reveal an increase in the size of these currents increase during embryonic maturation. It
573 is evident that the peak INa (V) varied across the sampled population at each age. We were
574 unable to reliably and systematically determine whether the variability reflected the presence of
575 cells of different sizes or whether the expression of INa (V) channels per unit of cell membrane
576 varied. Of note, Schmid & Guenther (1996) divided whole-cell sodium current amplitude by cell
577 capacitance and found that INa (V) current density increased sizably from E18 to P6.
578
579 Fig. 8 near here
580
581 **Electrophysiological recordings demonstrate that irradiance with light as dim as 3 x 10^{12}**
582 **photons/cm^2/s evoke responses in individual foetal mRGCs.**
583 Our previous work demonstrated that the ambient light in the mouse housing room was
584 bright enough to trigger subsequent vascular development via stimulation of melanopsin in the
585 eyes of foetal pups (Rao et al. 2013). Specifically, normal regression of the hyaloid blood
586 vessels was retarded in foetal pups lacking expression of melanopsin (*OPN4*$^{-/-}$) and in WT pups
587 whose mothers were dark-reared from 16.5 days post-conception to the time of the pups' birth.
588 The effects of ambient light were not transmitted from the pregnant female to the pups but were
589 a direct effect of ambient light on the foetal pups themselves. This was shown by the fact that
590 environmental light still contributed to normal ocular vessel development when the pregnant
591 female was enucleated or when melanopsin was selectively deleted in the pregnant mothers but
592 not in the foetal pups. Thus, the light that struck the foetal eyes resulted from ambient light
593 transmission through the abdominal walls of the dams. Direct measurements of the attenuation
594 of the intensity of blue light across the dams' skin and muscle layers support the notion that if
595 mRGCs in embryonic retinas are as sensitive to light as mRGCs in postnatal retinas, the
596 embryonic mRGCs could easily be activated by low-intensity environmental light at floor level in
597 the mouse housing room (5.6 x 10^{13} photons/cm^2/s, Rao et al. 2013). However, the actual
598 photosensitivity of embryonic mRGCs is unknown. In the GCaMP experiments described above
599 (Figs 2-7), we were not able to measure mRGC sensitivity because the minimum stimulus
600 intensity needed to interrogate GCaMPs strongly activated melanopsin as well. To circumvent
601 this experimental obstacle, we turned to a non-optical, electrophysiological approach using
602 patch pipette recordings from individual mRGCs.
603 We recorded light-evoked responses from fluorescently marked mRGCs in foetal retina
604 preparations. We found a total of 15 mRGCs that exhibited detectable light responses. Figure 9

605 shows light responses recorded from an mRGC in the retina of an E18.5 pup. Action potentials
606 were observed at an irradiance of 2.9 x 10^{12} photons/cm^2/s (Fig. 9D4). The onset of spiking
607 displayed a latency of 21 s. The responses to steps of light at higher irradiances (5.8 x 10^{14}, 1.5
608 x 10^{14} and 1.35 x 10^{13} photons/cm^2/s) are plotted in Fig. 9D1, D2, and D3, respectively. Similar
609 to the mRGC responses recorded in neonatal and adult retinas, the response latencies
610 decreased as the irradiance increased (Tu et al. 2005, Wong KW, 2012). In our sample of cells,
611 one mRGC had a threshold of 1.6 x 10^{12} photons/cm^2/s. Seven of the 15 mRGCs had
612 thresholds between 6.2 x 10^{12} and 3.5 x 10^{13} photons/cm^2/s, and six of the 15 light responders
613 had thresholds between 1.5 x 10^{14} and 2.4 x 10^{14} photons/cm^2/s. It should be noted that all of
614 the GCaMP6-expressing mRGCs recorded electrophysiologically were initially identified by their
615 responsiveness to light at 3.10^{17} – 3.10^{19} photons/cm^2/s (Fig. 9A,B).
616 A population of low-amplitude spikes during light onset and occasional depolarizing
617 "bumps" with a duration of approximately 1-2 s are evident in these recordings. We interpret the
618 smaller spikes as spikelets conducted from neighbouring mRGCs as described by Arroyo et al.
619 (2016). The bumps, which occur with a frequency of approximately 1/min, probably reflect the
620 occurrence of spontaneous waves (Meister et al. (1990); Maffei L& Galli-Resta L (1990)).
621
622 Figure 9 near here
623
624

625 **mRGCs in embryonic retinas are coupled via gap junctions.**

626 Cells in the adult mammalian retina are extensively coupled through gap junctions both
627 to cells of the same type and to cells of different types. In the retinas of rats and mice, in
628 particular, mRGCs are coupled to amacrine cells (Muller et al. 2010; Reifler et al. 2015).
629 However, dye coupling between mRGCs in adult rodent retina has not been found, although
630 Müller et al. (2010) and Ecker et al. (2010) specifically searched for homologous coupling
631 between these cells. Precedent suggests that gap junction coupling could be age-dependent
632 and that gap junction coupling may therefore exist in the retinas of younger mice. In spinal cord
633 (Walton and Navarrete, 1991) and in the cerebral cortex (Kandler and Katz, 1991), gap junction
634 coupling between neurons can exist early in development but is absent or much reduced in
635 older animals. Consistent with a greater prominence of gap junction coupling in the retinas of
636 very young animals compared to those of adults, Sekaran et al. (2003) reported that MFA, a
637 putative blocker of gap junction coupling, reduced the number of light-responsive cells in early
638 postnatal retinas. This was interpreted as evidence for gap junction coupling between mRGCs

639 and other cells. Subsequently, Arroyo et al. (2016) found MFA-inhibitable functional and tracer
640 dye coupling between genetically marked mRGCs in young neonatal mice (P4 to P8). We
641 extended the work of Arroyo et al. (2016) to specifically test whether prenatal mRGCs are
642 coupled to one another via gap junctions, pursuing the idea that younger mice may be more
643 likely to express gap junction communication. We tested whether MFA, a compound that is
644 commonly used to block gap junction coupling, reduced or eliminated light responses (Sekaran
645 et al. 2003; Veruki et al. 2010). We examined the effects of MFA on light-evoked calcium
646 elevations across a population of GCaMP-expressing mRGCs in fields of cells in flat-mounted
647 retinas. Figure 10A shows the combined results obtained from 81 cells in two separate E16.5
648 retinas. MFA reversibly attenuated the amplitudes of the cells' responses to light. The black dots
649 in the top panel plot the response amplitudes after washout as a function of the response
650 amplitudes observed prior to MFA application. The black dots are best fitted by a linear
651 regression corresponding to y = 1.04 x. The data show good recovery from MFA. The blue dots
652 plot the response amplitudes of each mRGC in MFA as a function of the response amplitudes
653 observed prior to MFA application. The best-fitted linear regression line is y = 0.21 x. Non-
654 parametric Wilcoxon Rank Sum Tests indicate that the reduction observed in MFA is highly
655 significant ($P = 8.3 \times 10^{-25}$). These results are consistent with the spreading of light-evoked
656 excitation between mRGCs via gap junctions. We performed the MFA experiments in 7 fields
657 from 5 embryonic retinas. In 4 fields, MFA attenuated the responses reversibly. In the other 3
658 fields, the light responses recovered to more than 80% of their pre-drug levels in only a minority
659 of the mRGCs. This apparent lack of reversibility is likely due to not having waited long enough
660 after initiating washout (> 20 min). It should also be noted that in *OPN4cre::Ai96* mice we could
661 only interrogate responses in mRGCs. Therefore, we were unable to use this method to rule out
662 gap junction coupling to other non-melanopsin-expressing neurons. Additionally, a caveat
663 associated with relying on MFA to identify gap junction coupling is that carbenoxolone, a
664 previously used MFA-related compound, has been reported to attenuate L-type calcium currents
665 in mRGCs (Bramley et al. 2011). Finding reduced numbers of light-responsive cells in MFA
666 could also be attributed to the reduction of calcium currents.
667 To explore whether our MFA findings did indeed indicate coupling between mRGCs, we
668 used patch pipettes to inject 17 embryonic mRGCs with neurobiotin as a means of tracing gap
669 junction-mediated dye coupling to adjacent cells. Figure 10B shows an example of an mRGC
670 that was injected with neurobiotin. Three somas were neurobiotin- and EGFP-positive, indicative
671 of migration of the tracer from one GCaMP6-expressing mRGC to at least two other mRGCs
672 (stars). At least five other somas were neurobiotin-positive (red) but lacked EGFP

673 immunoreactivity. In summary, in 12 of 17 injections, at least one nearby mRGC cell was filled
674 with neurobiotin. The maximum number of dye-coupled mRGCs observed to be connected an
675 injected mRGC was 4. In 10 of the 17 injected mRGCs, the axons were filled with neurobiotin.
676 Neurobiotin also filled from 0 to 7 non-mRGCs that were identified by the absence of OPN4cre-
677 driven EGFP or tdTomato from their cell bodies. We were often able to follow neurobiotin-filled
678 dendritic processes from the mRGC somas to the other dye-filled cells. These results provide
679 strong evidence that mRGCs are coupled to other mRGCs as well as to other classes of inner
680 retinal neurons in foetal mouse retinas.
681
682 **Figure 10** Near here
683
684

685 **Discussion**

686 The photopigment melanopsin is expressed in a subset of retinal ganglion cells termed
687 mRGCs. Markers for melanopsin first appear in embryonic mouse and human retinas well
688 before birth (embryonic day 11.5 and gestational week 8.6, respectively). mRGCs in postnatal
689 retinas can be excited autonomously by light independently of visual inputs from rods and
690 cones, the canonical photoreceptors in the eye. We recently demonstrated that exposure of
691 pregnant females to light regulates the normal maturation of ocular vasculature in subsequently
692 born pups. Based on our finding that the deletion of melanopsin in the foetal pups phenocopied
693 darkness, we inferred that light stimulation of mRGC in the eyes of the foetuses modulates
694 vascular maturation. There have been no reports directly demonstrating that mRGCs in foetal
695 retinas are light-sensitive, raising some doubts about whether the ambient light in the mouse
696 colony in which the pregnant females were housed was sufficient to excite mRGCs in the eyes
697 of the foetuses. Here, using both intracellular calcium indicators and patch pipette recordings,
698 we show that foetal mouse mRGCs respond to light as early as E15.5, four days before birth.
699 We report further that foetal mRGCs share many of the phototransduction pathways that have
700 been previously identified in mRGCs in the retinas of postnatal animals. Pharmacological
701 experiments reveal that light responses are initiated by the coupling of light-activated
702 melanopsin to a $G_{q/11}$-G-protein cascade. We also show that calcium influx through L-type
703 calcium channels and cation influx through TTX-sensitive sodium channels boost the amplitude
704 of photoresponses. Electrophysiological recordings from individual embryonic mRGCs
705 demonstrated that these cells can respond to light as dim as 2.9×10^{12} photons/cm^2/s, providing
706 strong supportive evidence that the ambient light in rooms where the pregnant females were

707 housed is sufficient to excite mRGCs in foetuses. Additionally, we found that when the dye
708 neurobiotin was injected into individual single mRGCs, it flowed into other nearby mRGCs via
709 gap junction coupling. This finding contrasts with reports performed in adult rodent retinas in
710 which no mRGC/mRGC coupling was discovered. Finding photosensitivity in the embryonic
711 retinas of mice raises the question of whether human foetuses and early preterm infants could
712 be sensitive to light and whether light exposure might modulate ocular development. Given that
713 light stimulation of mRGCs plays a role in entraining circadian rhythms and mood in postnatal
714 animals, some consideration should be given to the consequences of light exposure
715 experienced by human foetal or preterm infants. Light exposure sources might include lighting
716 regimens in neonatal care units and light exposure during intrauterine surgery. Such exposure
717 might influence ocular development and/or behavioural states.
718
719 **No evidence was found that other photopigment-expressing cells in the foetal retinas of**
720 **mice are light-sensitive.**
721 Could cells other than mRGCs in the embryonic eye confer light sensitivity that might
722 affect ocular development? The present study focussed on the light sensitivity of mRGCs in
723 retina. The results of the Calbryte 590™ experiments (Fig. 1) argue against the idea that OPN3-
724 and OPN5-expressing cells generate light responses in the foetal mouse retina. Strictly
725 speaking, we did not address the question of whether other non-retinal cell types that might
726 express melanopsin prenatally could regulate ocular development. However, the preponderance
727 of evidence presented here and in a previous study (Rao et al. 2013) strongly supports the idea
728 that light stimulation of mRGCs is sufficient to account for light modulation of ocular vasculature
729 maturation. In adult rodents, melanopsin expression has been found in the cornea, the iris and
730 the retinal pigmented epithelium (RPE). We recently showed that melanopsin-containing fibres
731 and cells in the corneas of postnatal animals were not light-responsive, suggesting that
732 melanopsin might play a role in other sensory modalities such as thermal detection (Delwig et
733 al. 2018). While light-sensitive melanopsin cells have been identified in the iris, there are no
734 reports that these cells are light-sensitive in embryonic retinas or even that melanopsin markers
735 are found in the embryonic irides. Melanopsin gene expression has been reported in cultured
736 lines derived from RPE. There is no evidence that native RPE or cultured RPE cells lines are
737 light-responsive. Further study focussed on the iris and RPE would be required to ascertain
738 whether light stimulation of these cell types alters the vascular maturation of the eye.
739
740 **mRGCs are coupled electrotonically to one another in the foetal retina.**

741 Syncytial networks of electrotonically coupled neurons facilitate the spread of excitation
742 across regions of neural tissue and coordinate the timing of excitability and rhythmic oscillations
743 (Nagy et al., 2018). Electrotonic coupling between heterologous and homologous classes of
744 neurons is common in both mammalian and non-mammalian neural tissues. Moreover, it is
745 commonly found that electrotonic coupling is more prominent in the tissues of younger animals
746 (Walton and Navarrete, 1991, Kandler and Katz, 1991). In the retinas of adult mice, electrotonic
747 coupling of mRGCs to other mRGCs seems to be absent [Müller et al. (2010), Ecker et al.
748 (2010)], but it is observed in younger postnatal mice (Sekaran et al. 2003; Arroyo et al. 2016). In
749 the present study, we found electrotonic coupling between mRGCs. Additionally, we have
750 evidence for electrotonic coupling from mRGCs to heretofore-unidentified non-mRGC cell types
751 in the inner retinas of foetal mice. Electrotonic coupling between mRGCs and other
752 heterologous neurons raises the possibility that light exposure during foetal and early postnatal
753 maturation could excite neighbouring ganglion cells that project axons to the higher visual
754 centres. In postnatal animals, light deprivation produced by suturing shut the eyelid of one eye
755 disturbs the normal segregation of eye-specific targets in higher visual centres. This suggests
756 that light excitation of mRGCs in neonatal animals before the normal age of eyelid opening may
757 play a previously unrecognized role in retinotopic mapping in the higher visual centres.
758 Another notion drawn from the results presented here is that foetal light exposure might
759 play a role in the formation of ocular dominance columns in primates. Horton and his colleague
760 (Horton & Hocking, 1996) found ocular dominance columns in newborn macaques that were
761 delivered by Caesarean section and kept in total darkness for a week after birth. Horton and
762 Hocking argued that the formation of columns was genetically programmed based on the
763 assumption that there had been no light-induced activity in the retinas of foetal monkeys. Given
764 our findings in mice, it is worth considering the idea that ambient light might stimulate mRGCs in
765 embryonic monkeys and thereby play a previously unrecognized role in the formation of ocular
766 dominance columns.
767
768 **Light excitation of mRGCs in foetal retinas could modify patterns of retinogeniculate**
769 **connections.**
770 Retinal ganglion cells extend axons to the lateral geniculate nucleus several days before
771 birth. The postsynaptic contact regions in the LGN exhibit eye-specific contact regions. A
772 consensus opinion is that spontaneous activity, often observed as propagated waves of activity,
773 plays a critical role in segregation (Shatz CJ & Stryker MP (1988); Shatz CJ (1996); Meister et
774 al. (1991); Maffei & Galli-Resta, (1990). Renna et al. (2011) and Arroyo et al. (2016) reported

775 that light modulated the temporal structure of retinal waves via activation of mRGCs in the
776 retinas of young neonatal mouse pups. Renna et al. (2011) also reported that mRGC excitation
777 perturbed the eye-specific targeting of RGC axons in the LGN. Given our demonstration that
778 light can activate mRGCs in foetal retina, we suggest that light exposure of pregnant females
779 might play a role in establishing retinogeniculate connectivity in the maturing pups. Light could
780 induce activity in mRGC axons targeting the LGN, or it could induce activity in neighbouring
781 RGCs that might be electrotonically coupled to mRGCs. Another alternative is that mRGC
782 excitation could modulate the structure of spontaneous waves that propagate across the foetal
783 retina. Further studies will be needed to establish whether the light-induced activity of mRGCs
784 as young as E15.5 is conducted to the LGN.
785
786 **Are human foetuses sensitive to light and might ambient lighting conditions at early**
787 **gestational ages affect eye development?**
788 Third-trimester human foetuses respond acutely to light directed through the mother's
789 abdominal wall. Examples of photic induced responses include modulation of heart rate and
790 body movement (Kiuchi et al. 2000) and visually evoked brain activity (Eswaran et al. 2004,
791 McCubbin et al. 2007). Since rods and cones begin functioning at approximately gestational
792 week 35, the acute actions of light stimulation could be activating rods and cones as well as
793 mRGCs. In any case, the occurrence of light-evoked responses in human foetuses
794 demonstrates that light can excite photoreceptors in the foetal eye after passing through the
795 abdominal wall of the pregnant mother.
796 Human eye development might also be sensitive to ambient light at gestational ages
797 near the end of the first trimester. Human foetuses at gestational day 60 are at the same
798 developmental age as mouse foetuses at gestational day 16.5 (Clancy et al. 2001), the age at
799 which ambient light modulates subsequent vascular maturation in mice. Relevant to the
800 possibility that reduced daily photoperiod might influence eye development in humans, an
801 analysis of 276,911 conscripts of the Israeli Defense Forces between 2000 and 2004 found an
802 association between an increased incidence of moderate and severe myopia and season of
803 birth. Conscripts for whom the end of the first *in utero* trimester occurred during the winter
804 months exhibited an increased risk of myopia (Mandel et al. 2008). One intriguing explanation is
805 that light exposure of foetuses during the first trimester influence eye growth. While Mandel et
806 al. (2008) ruled out family planning as a variable many other confounds need to be considered
807 including diseases experienced during winter months, Vitamin D deficiencies, birth weights and
808 other factors. In another analysis, Yang et al. (2013) reported that infants whose early gestation

occurred during the winter months were at increased risk of severe retinopathy of prematurity (ROP). These findings raise the possibility that ambient light passing across the abdominal wall of pregnant mothers early in gestation might be considered as a factor that could affect eye development.

References

Arroyo DA, Kirkby LA & Feller MB (2016). Retinal Waves Modulate an Intraretinal Circuit of Intrinsically Photosensitive Retinal Ganglion Cells. *J Neurosci*. 36:6892-905.

Arshavsky V.Y., Lamb T.D., Pugh E.N. Jr. (2002) G proteins and phototransduction. *Annu Rev Physiol*.; 64(): 153-87.

Bailes H.J. & Lucas R.J. (2013) Human melanopsin forms a pigment maximally sensitive to blue light (lambdamax approximately 479 nm) supporting activation of G(q/11) and G(i/o) signalling cascades. *Proc Biol Sci* 280(1759):20122987.

Berson D.M., Dunn F.A., Takao M. (2002) Phototransduction by retinal ganglion cells that set circadian clock. *Science*. 95:1070-3.

Bieda MC & Copenhagen DR (2004). N-type and L-type calcium channels mediate glycinergic synaptic inputs to retinal ganglion cells of tiger salamander. *Vis Neurosci.* 21:545-50.

Bramley JR, Wiles EM, Sollars PJ & Pickard GE. (2011) Carbenoxolone blocks the light-evoked rise in intracellular calcium in isolated melanopsin ganglion cell photoreceptors. *PLoS One*. 6(7):e22721. doi: 10.1371/journal.pone.0022721. Epub 2011 Jul 29.

Breedlove MA (2017) Foundations of Neural Development, Sinauer Associates, Sunderland, MA

Buhr ED, Yue WW, Ren X, Jiang Z, Liao HW, Mei X, Vemaraju S, Nguyen MT, Reed RR, Lang RA, Yau KW, & Van Gelder RN (2015) Neuropsin (OPN5)-mediated photoentrainment of local circadian oscillators in mammalian retina and cornea. *Proc Natl Acad Sci U S A* 112:13093-8.

Catterall WA, Perez-Reyes E, Snutch TP, Striessnig J. (2005) International Union of Pharmacology. XLVIII. Nomenclature and structure-function relationships of voltage-gated calcium channels. *Pharmacol Rev* 57:411-25.

Chen T.W., Chen TW, Wardill TJ, Sun Y, Pulver SR, Renninger SL, Baohan A, Schreiter ER, Kerr RA, Orger MB, Jayaraman V, Looger LL, Svoboda K. & Kim DS. (2013) Ultrasensitive fluorescent proteins for imaging neuronal activity. *Nature* 499(7458):295-300.

Chew K.S., Schmidt T.M., Rupp A.C., Kofuji P. & Trimarchi J.M. (2014) Loss of Gq/11 genes does not abolish melanopsin phototransduction. *PLoS One* 9(5):e98356.

855 Clancy B, Darlington RB & Finlay BL (2001) Translating developmental time across mammalian
856 species. *Neuroscience* 105:7-17.
857
858 Delwig A, Larsen DD, Yasumura D, Yang CF, Shah NM & Copenhagen DR (2016) Retinofugal
859 projections from melanopsin-expressing retinal ganglion cells revealed by intraocular
860 injections of cre-dependent virus. *PLoS One.* 11(2):e0149501. doi:
861 10.1371/journal.pone.0149501.
862
863 Delwig A, Chaney SY, Bertke AS, Verweij J, Quirce S, Larsen DD, Yang C, Buhr E, Van Gelder
864 R, Gallar J, Margolis T, Copenhagen DR. (2018) Melanopsin expression in the cornea. *Vis*
865 *Neurosci.* 35:E004. doi: 10.1017/S0952523817000359.
866
867 Do M.T.H. & Yau K.W. (2010) Intrinsically photosensitive retinal ganglion cells. *Physiol Rev*.
868 90:1547-81. doi: 10.1152/physrev.00013.2010.
869
870 Ecker JL, Dumitrescu ON, Wong KY, Alam NM, Chen SK, LeGates T, Renna JM, Prusky GT,
871 Berson DM & Hattar S (2010) Melanopsin-expressing retinal ganglion-cell photoreceptors:
872 cellular diversity and role in pattern vision. *Neuron* 67(1):49-60.
873
874 Eswaran H, Lowery CL, Wilson JD, Murphy P, & Preissl H (2004). Functional development of
875 the visual system in human fetus using magnetoencephalography. *Exp Neurol*. 190 Suppl
876 1:S52-8.
877
878 Graham DM, Wong KY, Shapiro P, Frederick C, Pattabiraman K & Berson DM. (2008)
879 Melanopsin ganglion cells use a membrane-associated rhabdomeric phototransduction
880 cascade. *J Neurophysiol* 99(5):2522-2532.
881
882
883 Hartwick AT, Bramley JR, Yu J, Stevens KT, Allen CN, Baldridge WH, Sollars PJ, Pickard GE
884 (2007) Light-evoked calcium responses of isolated melanopsin-expressing retinal ganglion
885 cells. *J Neurosci* 27(49):13468-13480.
886
887 Horton JC & Hocking DR (1996) An adult-like pattern of ocular dominance columns in striate
888 cortex of newborn monkeys prior to visual experience. *J Neurosci.* 16:1791-807.
889
890 Hughes S, Jagannath A, Hickey D, Gatti S, Wood M, Peirson SN, Foster RG & Hankins MW..
891 (2015) Using siRNA to define functional interactions between melanopsin and multiple G
892 Protein partners. *Cell Mol Life Sci* 72(1):165-179.
893
894 Johnston D & Wu S M-S. Foundations of Cellular Neurophysiology 1995, The MIT Press,
895 Cambridge Massachusetts
896
897 Johnson J, Wu V, Donovan M, Majumdar S, Rentería RC, Porco T, Van Gelder RN &
898 Copenhagen DR. (2010) Melanopsin-dependent light avoidance in neonatal mice. *Proc*
899 *Natl Acad Sci U S A* 107(40):17374-17378.
900

Kandler K, Katz, LC (1995). Neuronal coupling and uncoupling in the developing nervous system, *Curr. Opin. Neurobiol* 5, 98–105.

Katz B & Minke B. (2009) Drosophila photoreceptors and signaling mechanisms. *Front. Cell Neurosci.* 10.3389/neuro.03.002.2009.

Kawasaki T, Taniguchi M, Moritani Y, Hayashi K, Saito T, Takasaki J, Nagai K, Inagaki O & Shikama H. (2003) Antithrombotic and thrombolytic efficacy of YM-254890, a Gq/11 inhibitor, in a rat model of arterial thrombosis. *Thromb Haemost* 90(3):406-413.

Kiuchi M, Nagata N, Ikeno S & Terakawa N (2000) The relationship between the response to external light stimulation and behavioral states in the human fetus: how it differs from vibroacoustic stimulation. Early Hum Dev. 2000 May;58(2):153-65.

Kumbalasiri T. & Provencio I. (2005) Melanopsin and other novel mammalian opsins. *Exp Eye Res* 81(4):368-375.

Madisen L, Zwingman TA, Sunkin SM, Oh SW, Zariwala HA, Gu H, Ng LL, Palmiter RD, Hawrylycz MJ, Jones AR, Lein E & Zeng H. (2010) A robust and high-throughput Cre reporting and characterization system for the whole mouse brain. *Nat Neurosci* 13(1):133-140.

Maffei L & Galli-Resta (1990) Correlation in the discharges of neighboring rat retinal ganglion cells during prenatal life *Proc Natl Acad Sci USA* 87:2861-4.

Mandel Y, Grotto I, El-Yaniv R, Belkin M, Isreal E, Polat U & Bartov E. (2008) Season of birth, natural light, and myopia. *Ophthalmology*. 115:686-92. Epub 2007 Aug 15.

McNeill DS, Sheely CJ, Ecker JL, Badea TC, Morhardt D, Guido W & Hattar S. (2011) Development of melanopsin-based irradiance detecting circuitry. *Neural Dev*. 6:8. doi: 10.1186/1749-8104-6-8.

Melyan Z, Tarttelin EE, Bellingham J, Lucas RJ & Hankins MW (2005) Addition of human melanopsin renders mammalian cells photoresponsive. *Nature* 433(7027):741-745.

Meister M, Wong RO, Baylor DA & Shatz CJ.(1991) Synchronous bursts of action potentials in ganglion cells of the developing mammalian retina. *Science* 252:939-43.

McCubbin J, Murphy P, Eswaran H, Preissl H, Yee T, Robinson SE & Vrba J. (2007) Validation of the flash-evoked response from fetal MEG. *Phys Med Biol.* 52:5803-13. Epub 2007 Sep 10.

946 Morin L.P., Blanchard J.H. & Provencio I. (2003) Retinal ganglion cell projections to the hamster
947 suprachiasmatic nucleus, intergeniculate leaflet, and visual midbrain: bifurcation and
948 melanopsin immunoreactivity. *J Comp Neurol* 465(3):401-416.
949
950 Müller LP, Do MT, Yau KW, He S and Baldridge WH. (2010) Tracer coupling of intrinsically
951 photosensitive retinal ganglion cells to amacrine cells in the mouse retina. *J Comp Neurol*.
952 518:4813-24.

953 Nagy JI, Pereda AE & Rash JE (2018). Electrical synapses in mammalian CNS: Past eras,
954 present focus and future directions*. Biochim Biophys Acta Biomembr.* 1860:102-123. doi:
955 10.1016/j.bbamem.2017.05.019. Epub 2017 Jun 1.

956 Newman LA, Walker MT, Brown RL, Cronin TW & Robinson PR (2003) Melanopsin forms a
957 functional short-wavelength photopigment *Biochemistry* 42:12734-8.
958
959 Nishimura A, Kitano K, Takasaki J, Taniguchi M, Mizuno N, Tago K, Hakoshima T, Itoh H.
960 (2010) Structural basis for the specific inhibition of heterotrimeric Gq protein by a small
961 molecule, *Proc Natl Acad Sci U S A* 107: 13666-13671.
962
963 Nguyen MT, Vemaraju S, Nayak G, Odaka Y, Buhr ED, Alonzo N, Tran U, Batie M, Upton BA,
964 Darvas M, Kozmik Z, Rao S, Hegde RS, Iuvone PM, Van Gelder RN & Lang RA. (2019)
965 An opsin-5 dopamine pathway mediates light-dependent vascular development in the eye.
966 *Nat Cell Biol.* 21:420-429. doi: 10.1038/s41556-019-0301-x. Epub 2019 Apr 1.
967
968 Panda S, Provencio I, Tu DC, Pires SS, Rollag MD, Castrucci AM, Pletcher MT, Sato TK,
969 Wiltshire T, Andahazy M, Kay SA, Van Gelder RN & Hogenesch JB. (2003) Melanopsin is
970 required for non-image-forming photic responses in blind mice. *Science* 301(5632):525-
971 527.
972
973 Panda S, Sato TK, Castrucci AM, Rollag MD, DeGrip WJ, Hogenesch JB, Provencio I & Kay
974 SA. (2002) Melanopsin (Opn4) requirement for normal light-induced circadian phase
975 shifting. *Science* 298(5601):2213-2216.
976
977 Panda S*,* Nayak SK, Campo B, Walker JR, Hogenesch JB & Jegla T. (2005) Illumination of the
978 melanopsin signaling pathway. *Science* 307(5709):600-604.
979
980 Provencio I., Jiang G., De Grip W.J., Hayes W.P. & Rollag M.D. (1998) Melanopsin: An opsin in
981 melanophores, brain, and eye. *Proc Natl Acad Sci U S A* 95(1):340-345
982
983 Qiu X*,* Kumbalasiri T, Carlson SM, Wong KY, Krishna V, Provencio I & Berson DM. (2005)
984 Induction of photosensitivity by heterologous expression of melanopsin. *Nature*
985 433(7027):745-749.
986

987 Rao S, Chun C, Fan J, Kofron JM, Yang MB, Hegde RS, Ferrara N, Copenhagen DR & Lang
988 RA. (2013) A direct and melanopsin-dependent fetal light response regulates mouse eye
989 development. *Nature* 494(7436):243-246.
990
991 Reifler AN, Chervenak AP, Dolikian ME, Benenati BA, Li BY, Wachter RD, Lynch AM,
992 Demertzis ZD, Meyers BS, Abufarha FS, Jaeckel ER, Flannery MP, Wong KY. (2015) All
993 Spiking, Sustained ON Displaced Amacrine cells receive Gap-Junction Input from
994 Melanopsin Ganglion Cells. *Curr Biol* 25:2878.
995
996 Renna JM, Wang S & Berson DM (2011) Light acts through melanopsin to alter retinal waves
997 and segregation of retinogeniculate afferents. *Nat Neurosci*. *14*:827-9.
998
999 Rörig B & Grantyn R (19914) Ligand- and voltage-gated ion channels are expressed by
1000 embryonic mouse retinal neurones Neuroreport. 5:1197-1200.
1001
1002 Schrage R, Schmitz AL, Gaffal E, Annala S, Kehraus S, Wenzel D, Büllesbach KM, Bald T,
1003 Inoue A, Shinjo Y, Galandrin S, Shridhar N, Hesse M, Grundmann M, Merten N,
1004 Charpentier TH, Martz M, Butcher AJ, Slodczyk T, Armando S, Effern M, Namkung Y,
1005 Jenkins L, Horn V, Stößel A, Dargatz H, Tietze D, Imhof D, Galés C, Drewke C, Müller CE,
1006 Hölzel M, Milligan G, Tobin AB, Gomeza J, Dohlman HG, Sondek J, Harden TK, Bouvier
1007 M, Laporte SA, Aoki J, Fleischmann BK, Mohr K, König GM, Tüting T, Kostenis E. (2015)
1008 The experimental power of FR900359 to study Gq-regulated biological processes. *Nature*
1009 *communications* 6:10156.
1010
1011 Sekaran S, Lupi D, Jones SL, Sheely CJ, Hattar S, Yau KW, Lucas RJ, Foster RG & Hankins
1012 MW. (2005) Melanopsin-dependent photoreception provides earliest light detection in the
1013 mammalian retina. *Curr Biol* 15(12):1099-1107.
1014
1015 Sekaran S, Foster RG, Lucas RJ, & Hankins MW (2003) Calcium imaging reveals a network of
1016 intrinsically light-sensitive inner-retinal neurons. *Curr Biol* 13(15):1290-1298.
1017
1018 Schmid S, Guenther E. (1996) Developmental regulation of voltage-activated Na+ and Ca2+
1019 currents in rat retinal ganglion cells. *Neuroreport*. 7:677-81.
1020
1021 Schmidt TM, Taniguchi K, Kofuji P. (2008) Intrinsic and extrinsic light responses in melanopsin-
1022 expressing cells during mouse development *J Neurophysiol.* 100:371-84. doi:
1023 10.1152/jn.00062.2008. Epub 2008 May 14
1024
1025 Shatz CJ & Stryker MP (1988) Prenatal tetrodotoxin infusion blocks segregation of
1026 retinogeniculate afferents. *Science* 242:87-9;
1027
1028 Shatz CJ (1996) Emergence of order in visual system development. *Proc Natl Acad Sci USA*
1029 23:602-8.
1030

1031 Singer JH, Mirotznik RR, Feller MB. (2001) Potentiation of L-type calcium channels reveals
1032 nonsynaptic mechanisms that correlate spontaneous activity in the developing mammalian
1033 retina. *J Neurosci.* 21:8514-22.
1034
1035
1036 Taniguchi M, Suzumura K, Nagai K, Kawasaki T, Takasaki J, Sekiguchi M, Moritani Y, Saito T,
1037 Hayashi K, Fujita S, Tsukamoto S & Suzuki K. (2004) YM-254890 analogues, novel cyclic
1038 depsipeptides with Galpha(q/11) inhibitory activity from Chromobacterium sp. QS3666.
1039 *Bioorg Med Chem* 12(12):3125-3133.
1040
1041 Tarttelin EE, Bellingham J, Bibb LC, Foster RG, Hankins MW, Gregory-Evans K, Gregory-Evans
1042 CY, Wells DJ & Lucas RJ. (2003) Expression of opsin genes early in ocular development
1043 of humans and mice. *Exp Eye Res* 76(3):393-396.
1044
1045 Tischbirek C, Birkner A, Jia H, Sakmann B, & Konnerth A. (2015) Deep two-photon brain
1046 imaging with a red-shifted fluorometric Ca2+ indicator. *Proc Natl Acad Sci U S A*.
1047 112:11377-82. doi: 10.1073/pnas.1514209112. Epub 2015 Aug 24.
1048
1049 Tu D*C,* Zhang D, Demas J, Slutsky EB, Provencio I, Holy TE & Van Gelder RN. (2005)
1050 Physiologic diversity and development of intrinsically photosensitive retinal ganglion cells.
1051 *Neuron* 48(6):987-999.
1052

1053 Vemaraju S, Nayak G, , Miller WE, Copenhagen DR & Lang RA (2019) Fetal stage melanopsin
1054 (OPN4) and GNAQ (Gαq) signaling regulates vascular development of the eye *BioRxiv*
1055 doi: https://doi.org/10.1101/537225

1056
1057 Veruki ML, Oltedal L & Hartveit E (2010). Electrical coupling and passive membrane properties
1058 of AII amacrine cells. *J. Neurophysiol* 103, 1456-66. doi: 10.1152/jn.01105.2009. Epub
1059 2010 Jan 20.
1060
1061
1062 Walton KD, Navarrete R (1991). Postnatal changes in motoneurone electrotonic coupling
1063 studied in the *in vitro* rat lumbar spinal cord *J Physiol*. 433, 283-305.
1064
1065 Wong KY (2012) A retinal ganglion cell that can signal irradiance continuously for 10 hours. *J*
1066 *Neurosci* 32(33):11478-11485.
1067
1068 Wettschureck N, Rütten H, Zywietz A, Gehring D, Wilkie TM, Chen J, Chien KR & Offermanns
1069 S. (2001) Absence of pressure overload induced myocardial hypertrophy after conditional
1070 inactivation of Galphaq/Galpha11 in cardiomyocytes. *Nat Med* 7(11):1236-1240.
1071
1072 Yang MB, Rao S, Copenhagen DR & Lang RA (2013) Length of day during early gestation as a
1073 predictor of risk for severe retinopathy of prematurity. *Ophthalmology* 120:2706-2713.

Yasui F, Miyazu M, Yoshida A, Naruse & Takai A. (2008) Examination of signalling pathways involved in muscarinic responses in bovine ciliary muscle using YM-254890, an inhibitor of the Gq/11 protein. *Br J Pharmacol.* 154(4):890-900. doi: 10.1038/bjp.2008.140. Epub 2008 Apr 21.

Zariwala HA, Borghuis BG, Hoogland TM, Madisen L, Tian L, De Zeeuw CI, Zeng H, Looger LL, Svoboda K & Chen TW. (2012) A Cre-dependent GCaMP3 reporter mouse for neuronal imaging in vivo. *J Neurosci* 32(9):3131-3141.

Zhao Q, Guo H, Ruggu P, Jixiang, L, Liao J & Diwu, Z (2019) New Red Fluorescent Calcium Indicators for Functional Analysis of GPCRs and Ca2+ Channel Targets. *Biophysical Journal* (2019): 240a

Zheng W, Rampe D & Triggle DJ (1990) Pharmacological, radio ligand binding, and electrophysiological characteristics of FPL 64176, a novel nondihydropyridine Ca2+ channel activator, in cardiac and vascular preparations. *Mol Pharmacol* 40:734-41.

Biographies

Jan Verweij acquired his doctorate in neuroscience at the University of Amsterdam under the mentorship of Martin Kammermans, where he studied synaptic and electrotonic interaction between rods and cones in goldfish retina]. He joined the laboratory of Denis Dacey at the University of Washington, where he studied synaptic interactions in monkey retina. Then, he joined the laboratory of Julie Schnapf at UCSF to study functional interactions between rods and cones in monkey retina.

Shawnta Y. Chaney received her B.S. in Biology and her Ph.D. in Biochemistry at the University of Houston, Houston TX. There, she studied the effects of gestational lead (Pb2+) exposure on mouse retinas. She further studied retinal development as a postdoctoral scholar in David Copenhagen's lab at UCSF, where she focussed on embryonic and early postnatal light activation of melanopsin ganglion cells. Shawnta is now an Ocular Scientist at UNITY Biotechnology, where she tests therapies for age-related ocular diseases.

Additional information

Competing interests

The authors declare that they have no competing interests.

Author contributions

DRC and RAL provided project leadership. JV, SYC, DRC and DB and designed and performed experiments and analysed data. DRC wrote the manuscript. JV, SYC, DB, SV and RAL critiqued the study and edited the manuscript. GMK, EK provided crucial reagents and advice.

Funding

Funding was provided by the following sources: National Eye Institute (R01 EY02636 to RAL and DRC; R01 EY 01869 to DRC, R21 EY025435 to DRC, P30 EY002162 to UCSF) Ophthalmology, Additional support was provided by That Man May See (San Francisco), an unrestricted grant from Research to Prevent Blindness (UCSF Ophthalmology) and the German research foundation- (DFG) funded research unit FOR2372, projects no. 1582/10-1, KO 1582/10-2 to E.K. and G.M.K.

Acknowledgements

We thank Anton Delwig and Michael Stryker for valuable discussion and advice during the course of this research. We thank Andrew Ishida for his critique of the manuscript. For technical advice, we thank Franklin Caval-Holme, James Bothelo III, Travis Porco and Jessica Wong.

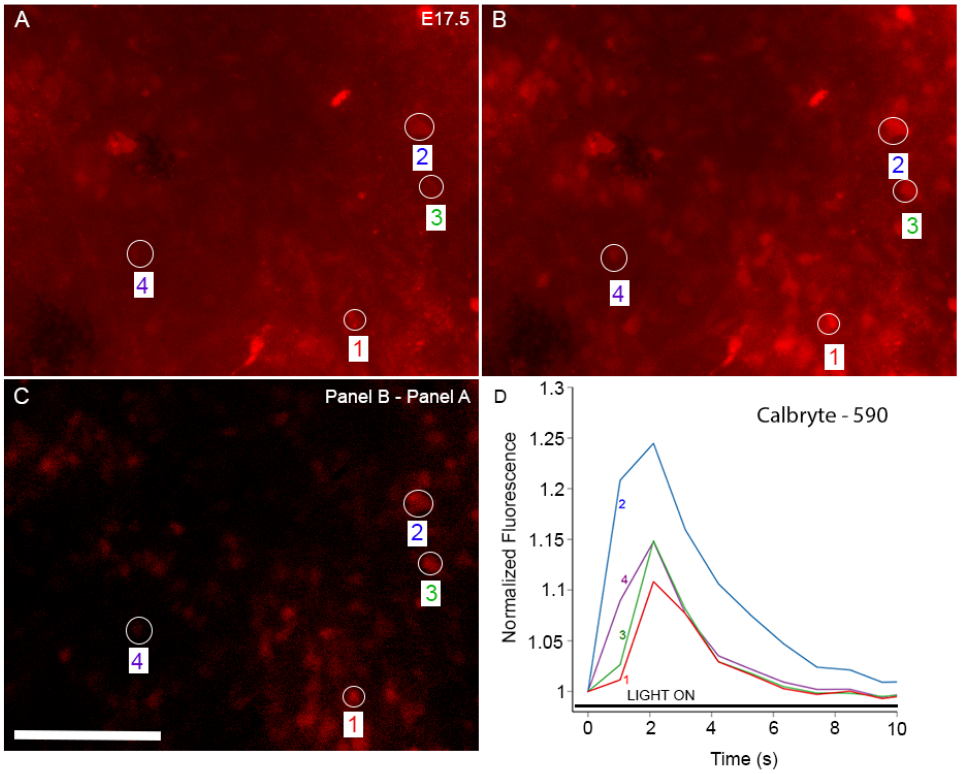

Figure 1 Cells in foetal mouse retinas are light-responsive.

Cells in embryonic mouse retinas exhibit light-dependent increases in intracellular calcium. (A-C) Representative images of light-evoked fluorescence recorded from cells in an isolated, flat-mounted retina of an E17.5 mouse after loading of the retina with Calbryte-590 calcium-sensing dye. Images of a 340 x 430 mm region of the retina captured at T=0 s and at T = 2.5 s (A, B) are displayed. The colour-coded regions of interest (ROIs) show 4 cells in which light evoked a very discernible increase in fluorescence, indicating an increase in intracellular calcium. (C) Difference image of the two frames ($T_{2.5} – T_0$) highlighting the regions in which increased dye fluorescence was observed after light onset. (D) Plots of the temporal response profiles of the cells marked by ROIs. The ordinate plots dF/F, where F is the baseline fluorescence immediately after the onset of the stimulus and prior to the onset of the response. Stimulus light of 480 nm wavelength was applied at 4 x 10^{17} photons/cm^2/s. The scale bars in A, B and C indicate 50 μm.

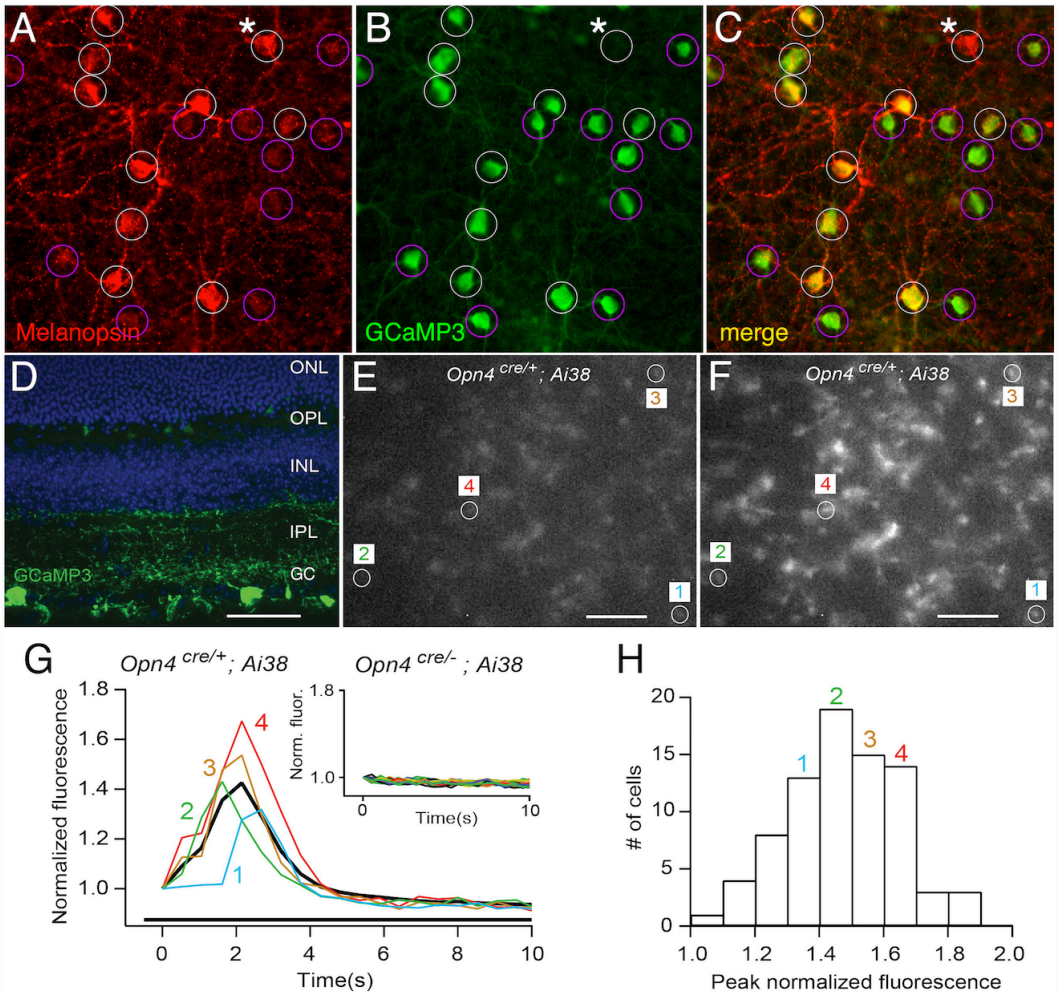

Figure 2. The genetically encoded intracellular calcium indicator GCaMP3 reveals light responses of melanopsin RGCs in embryonic retinas. Retinas from melanopsin knockout mice were unresponsive to light.

GCaMP3-EGFP co-localizes with melanopsin and indicates light responsiveness of foetal mRGCs in *Opn4*$^{cre/+}$::Ai38 retinas. (A) A flat-mount retina from an *Opn4*$^{cre/+}$*::Ai38* postnatal day 7 (P7) pup showing its melanopsin immunoreactivity (red). (B) GCaMP3-EGFP-immunoreactive cells (green). (C) Merged image of (A) and (B). The white circles show co-labelled cells; the purple circles mark cells in which GCaMP3^{+} immunoreactivity is strong and melanopsin immunoreactivity is absent or very dim. White circles with an asterisk mark the occasional melanopsin+, GCaMP3-negative cells. These particular cells probably reflect failure of the GCaMP3 allele to recombine. (D) GCaMP3-EGFP immunoreactivity in a perpendicular cryosection of P30 retina. Immunoreactivity is observed in the ganglion cell layer (GC), the inner plexiform layer (IPL) and within a few structures in the outer plexiform layer (OPL). (E, F) Retinas isolated from embryonic pups were placed in a perfusion chamber and stimulated with 480 nm light. (E) GCaMP3 fluorescence at the onset of the light response in one representative E16.5 retina. (F)

Fluorescence recorded at the peak of the light response in the same retina. Visual comparison of the images in (E) and (F) shows qualitatively brighter images in (F). (G) Time course of light-induced increases in df/F for 4 light-responsive cells (numbered 1 to 4 and colour-coded). The thick black trace plots the average response of 79 light-responsive cells in this experiment. These plots allow a more quantitative comparison of light responses in individual mRGCs. The scale bars indicate 50 μm. (G inset) Deletion of melanopsin (genotype *Opn4*$^{cre/cre}$*::Ai38*) reveals, first, that melanopsin is required for light responses and, second, that the observed light-evoked increases in fluorescence do not result from unrecognized effects of light on GCaMP3-EGFP.

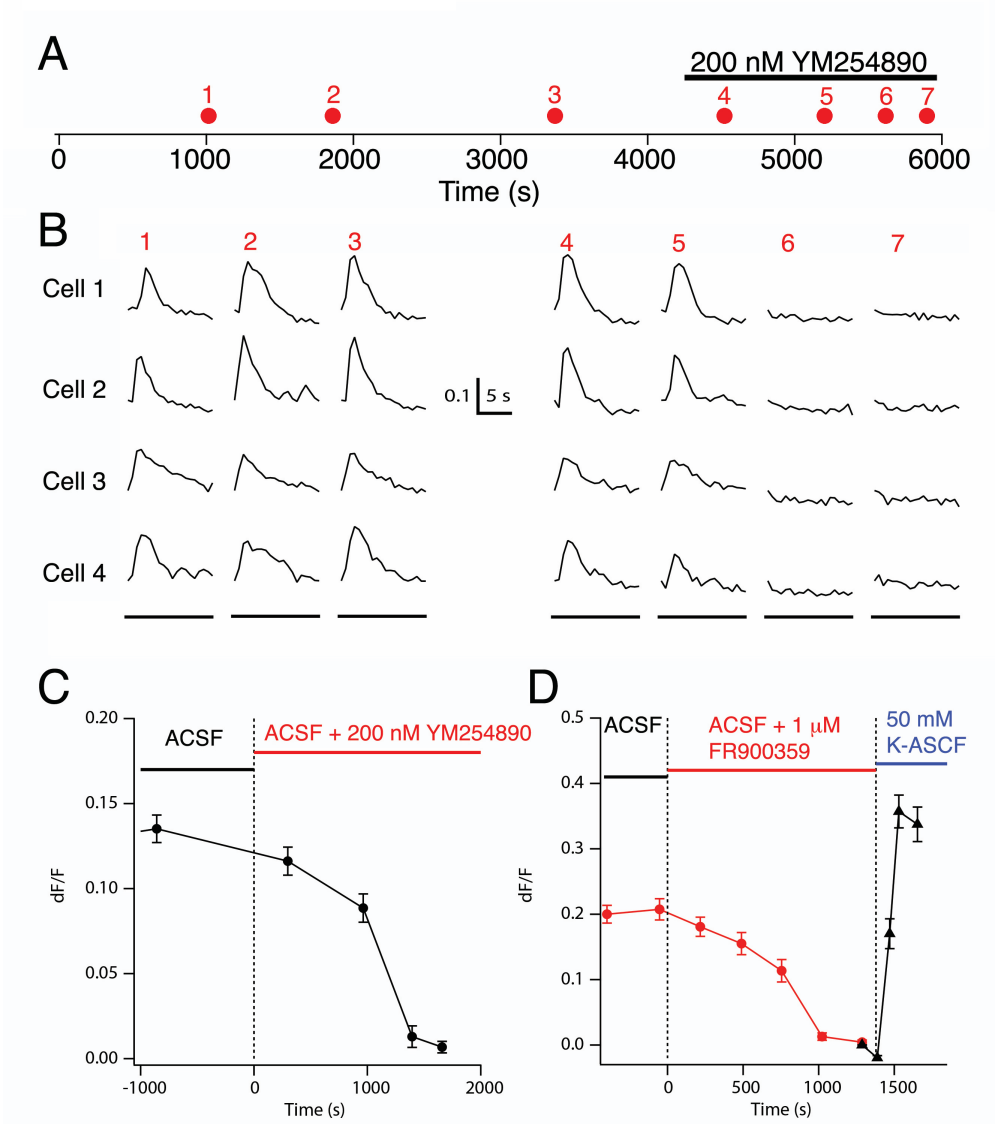

Figure 3. Antagonists that block the functions of the Gnaq, Gna11 and Gna14 alpha subunits of $G_{q/11}$-G **proteins of the $G_{q/11}$ family severely attenuate the light responses of mRGCs in foetal retinas.**

The effects of YM-254890 (200 nM) and FR900359 (1 μM), two different antagonists of Gnaq, Gna11 and Gna14, on light-evoked calcium elevations were tested in 4 explanted E15.5 and 3 explanted E16.5 OPN4cre::Ai96 retinas. (A) Time course of the experiment in an E16.5 retina showing 12-s light stimuli (red dots, 1-7) over the course of 6000 s. Responses to light stimuli 1-3 were recorded during 3300 s in control ACSF, and responses to light stimuli 4-7 were recorded after application of YM-254890. (B) Selected light responses from 4 mRGCs before and during perfusion with YM-254890. The scale bar shows df/F of 0.1. (C) Mean response amplitudes observed in 32 simultaneously recorded mRGCs in the same E15.5 retina analysed in (B). (D) Mean response amplitudes observed in 43 simultaneously recorded mRGCs in an E16.5 retina

perfused with medium containing 1 mM FR900359 (from ~400 to 1800 s). When dF/F responses were close to zero at 1400 seconds, the retina was perfused with 50 mM K-ACSF in which 47.5 mM NaCl was substituted for 47.5 mM KCl. The inclusion of KCl in the ACSF increased the calcium fluorescent signals to a level brighter than that induced by light before perfusion with FR9000359. All of the cells plotted in (C) and (D) had an initial criterion light response dF/F > 0.05. The error bars indicate the SEM.

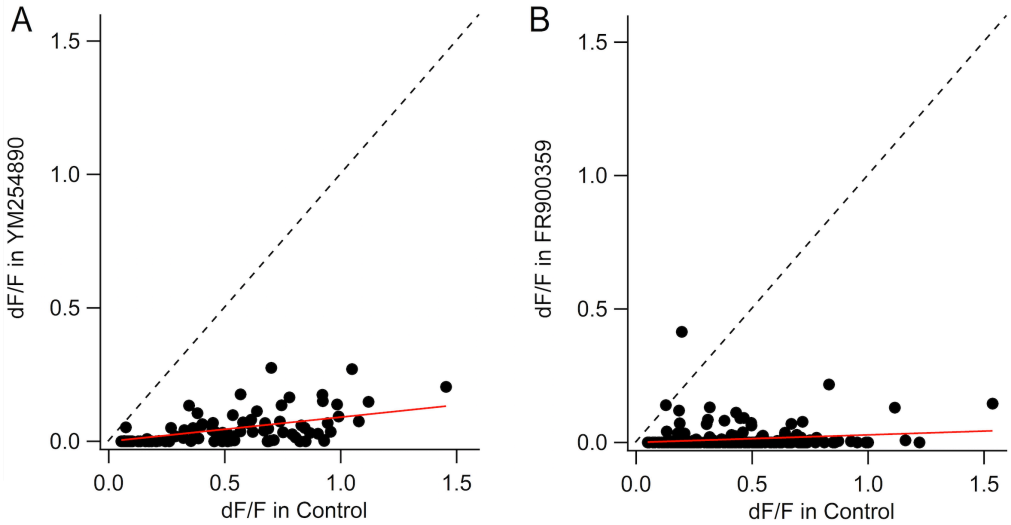

Figure 4 Ensemble data confirming that YM254890 and FR900359 uniformly attenuate light responses in virtually all embryonic mRGCs.

(A) Combined light-evoked dF/F's of 93 cells from E15.5 and E16.5 *OPN4cre::Ai96* retinas. All cells had a light-evoked dF/F > 0.05 in control conditions. The black dots indicate the lowest dF/F after 1500-2500 s incubation in 200 nM YM-254890 versus control dF/F for each cell. Prolonged incubation in 200 nM YM-254890 reduced the average dF/F of the light responses to 7% ± 11% that of the control responses (n=93). The data are best fitted by the linear regression y = 0.09x (solid red line). The dashed line indicates the predicted location of the dots if YM-254890 had no effect. (B) Combined light-evoked dF/F's of 219 cells from 3 embryonic day 16.5 retinas. All cells exhibited dF/F > 0.05 under control conditions. The black dots indicate the lowest dF/F after a 1300-3100 s incubation in 1 mM FR900359 versus control dF/F for each cell. Prolonged incubation in 1 mM FR900359 reduced the average dF/F of the light responses to 4% ± 18% that of the control responses (n=219). The data are best fitted by the linear regression y = 0.03x (solid red line). These results are highly significant (Wilcoxon Signed Rank Test for paired data [two-tailed P = $2.01948e^{-028}$ for YM and even smaller for FR]).

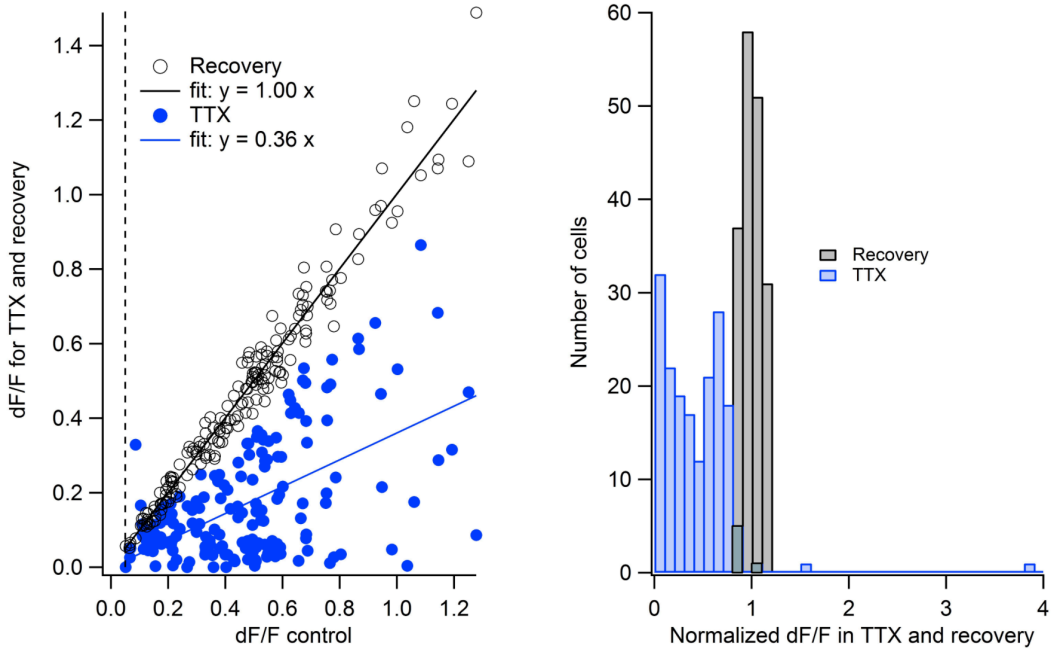

Figure 5 TTX variably but reversibly reduces the amplitude of light responses across the population of embryonic mRGCs.

(A) We measured the action of TTX on the fluorescent light responses of GCaMP6-expressing mRGCs in *OPN4cre::Ai96* embryonic retinas. Combined data from 4 E16.5 retinas are shown. The criteria for selecting each cell were that dF/F in control ACSF was > 0.05 and that the response amplitude after TTX washout recovered to between 80% and 120% of the control value. The open circles plot the recovery dF/F versus control dF/F for each of the 177 light-responsive mRGCs. The solid blue dots plot dF/F in 1 μM TTX versus control dF/F for each cell. The black line (y = 1.00 x) indicates the best-fitting linear regression line through the recovery data and the origin 0,0. The blue line (y = 0.36 x) is the best-fitting linear regression line for the TTX data. The differences between the results obtained during TTX treatment and under control conditions are highly significant (Wilcoxon Signed Rank Test for paired data, two-tailed P = $1.01e^{-46}$). (B) Histogram of the data shown in (A). The blue bars plot dF/F in TTX divided by the dF/F under control conditions, and the grey bars plot dF/F in recovery divided by the dF/F under control conditions.

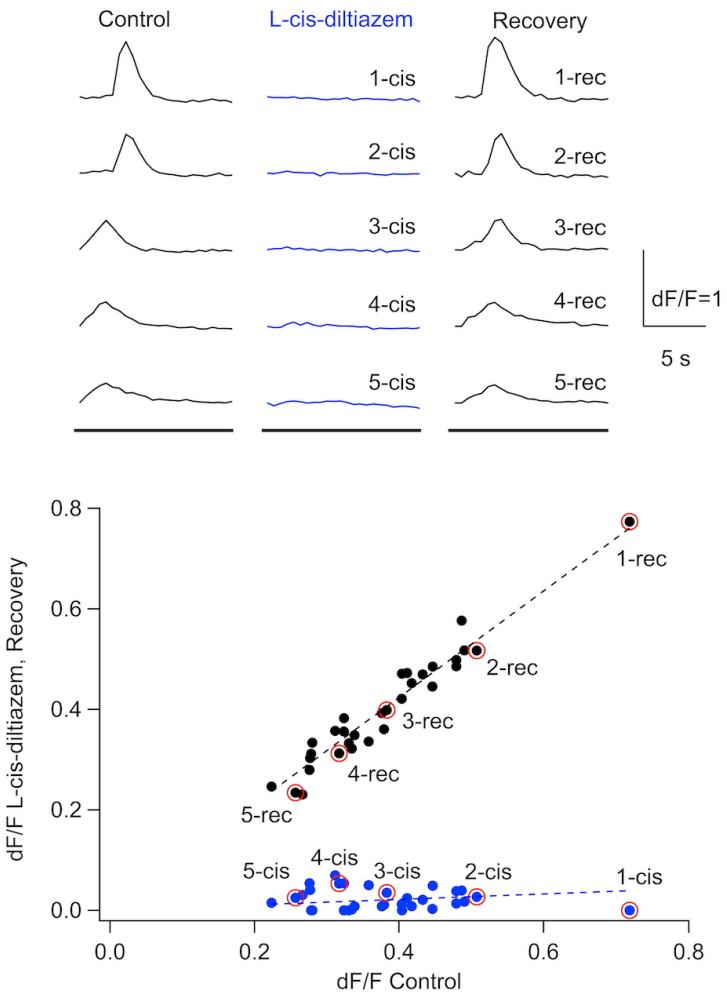

Figure 6 The L-type calcium channel antagonist L-cis-diltiazem (LCD) reversibly attenuates light-dependent increases in calcium in E16.5 mRGCs

(A) dF/F versus time in control ACSF, in LCD and after return to ACSF. Plots show representative recordings for 5 of 48 light-responsive cells from a single E16.5 *OPN4cre::Ai96* retina. The bars at the bottom indicate the timing of the light stimuli. (B) Plots of dF/F in LCD and recovery versus dF/F in control for 31 of 48 light-responsive cells in one retina in which the post-washout values recovered to between 80 and 120% of the control values. The dotted lines show the best linear regression that fits the data (y = 1.06x and y = 0.05x for recovery and LCD, respectively). The data from the 5 cells shown in (A) are shown as red circles. The Wilcoxon Rank Test for paired data yields a two-tailed P-value of $9.31323e^{-10}$, indicating that L-cis-diltiazem at 25 μM highly significantly diminishes light responses in mRGCs.

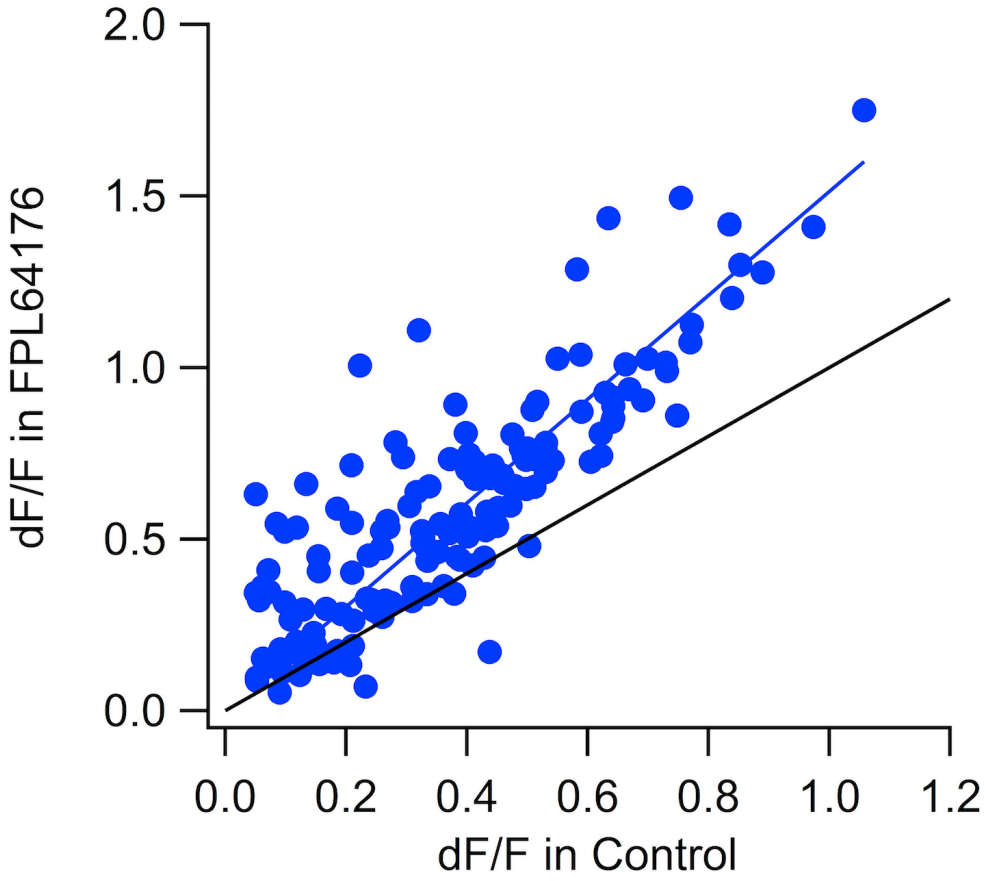

Figure 7 The L-type calcium channel agonist FPL64176 increases light- evoked dF/Fs recorded from embryonic mRGCs.

A) dF/F in 2 mM FPL64176 versus dF/F in control for 147 mRGCs combined from 2 E16.5 *OPN4cre::Ai96* retinas. The blue line represents the best linear regression fit: y = 1.51x. The black line represents the parity of response in control and FPL64176. The Wilcoxon Rank test for paired data yielded a two-tailed P-value of $1.17193e^{-32}$, indicating that dF/F is very significantly larger during exposure of the mRGCs to FPL64176 than under control conditions. No recovery data are shown, as FPL washout is known to be very poor (Bieda and Copenhagen, 2004).

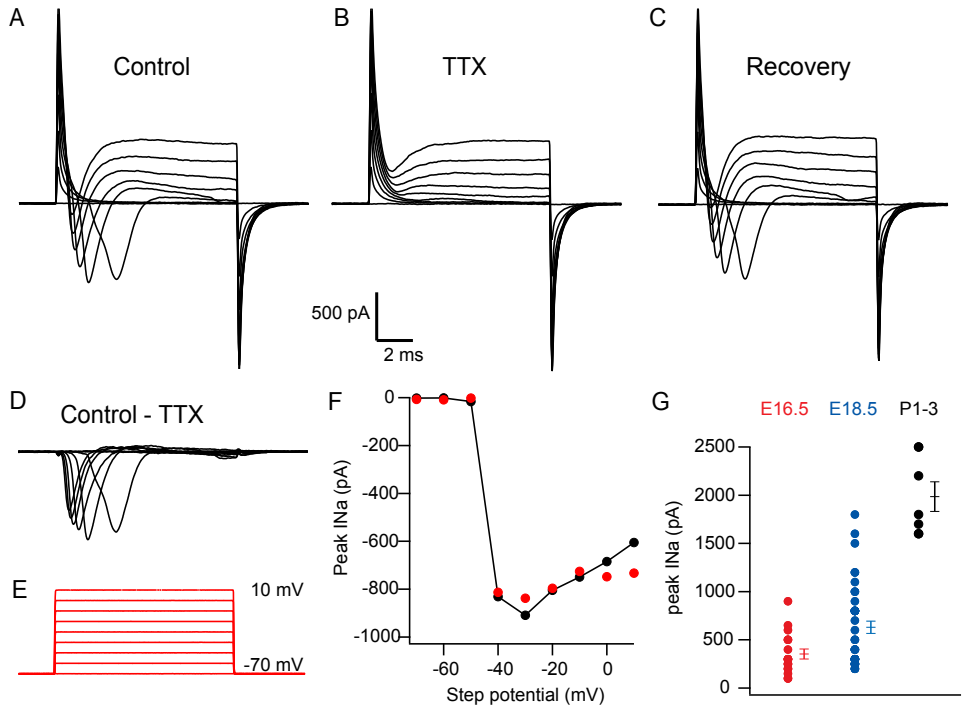

Figure 8 Patch pipette recordings reveal that TTX-sensitive sodium currents in mRGCs increase in amplitude during maturation from E16.5 to P1-3.

A-F show examples of TTX-sensitive currents recorded from an mRGC in an E18.5 retina (*OPN4cre::Ai96*) under voltage clamp conditions. A) Currents evoked under control conditions with the voltage clamp protocol shown in E. B) Currents evoked after several minutes in 1 μm TTX. C) Currents evoked after washout of TTX. D) Difference current, Control - TTX. E) Voltage clamp step protocol. F) The black dots indicate the maximum inward current for each trace from D versus the step potential (measurement of INa(V). To survey the amplitudes of peak Ina(V) across multiple cells in retinas of 3 different ages without applying TTX, we used an analytical method in which the final current sample of the voltage step in A was subtracted from the lowest current amplitude across the entire voltage step. These values, plotted as red dots, yield a good estimate of peak INa(V), as shown by comparison with the results obtained in TTX (black dots). G) Peak sodium currents in mRGCs during embryonic maturation. The dots indicate peak INa(V) estimates for 10, 35 and 7 mRGCs recorded from E16.5, E18.5 and P1-3 retinas, respectively. The vertical bars indicate the average ± standard error for each age (320 ± 73, 674 ± 72 and 1986 ± 153 pA, respectively). The data include whole-cell and perforated recordings and were not corrected for series resistance. In summary, these findings demonstrate that voltage-activated sodium currents are evident in

mRGCs at least 4 days before birth and that the magnitude of these currents increases with age.

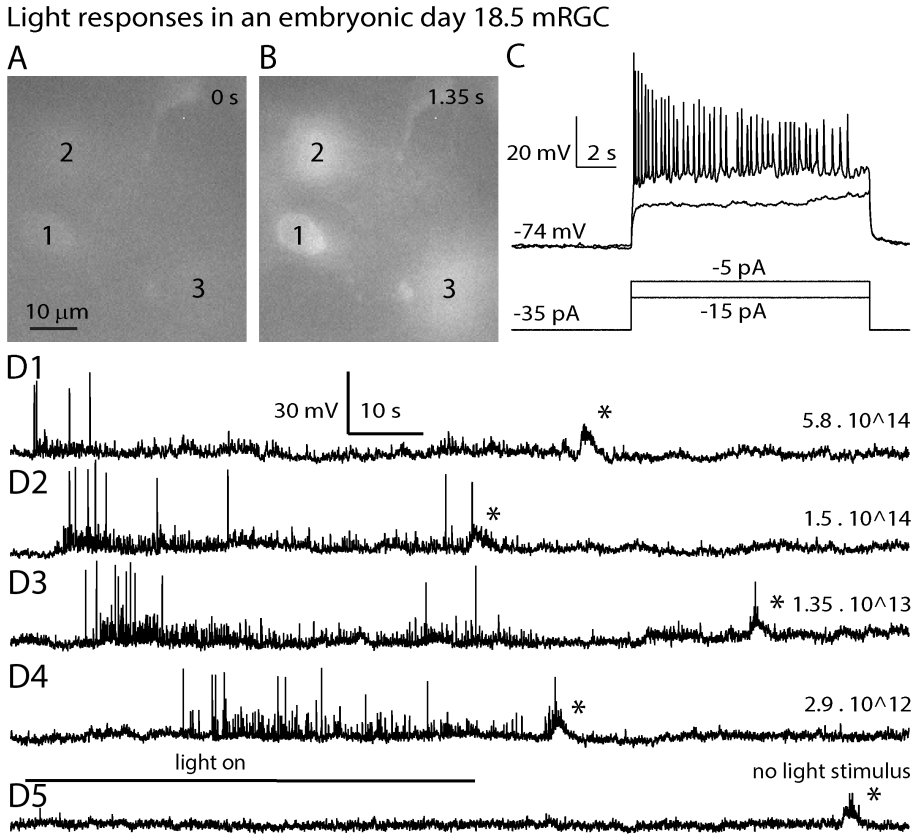

Figure 9

Light responses recorded from an mRGC in the retina of a foetal (E18.5) mouse pup.

To select mRGCs for electrophysiological patch pipette recordings, we first surveyed the retina for light-induced calcium responses, which should be restricted to melanopsin cells (OPN4cre::Ai96). Then, using infrared Nomarski imaging, we searched for light-responsive mRGCs whose cell bodies were exposed on the inner surface of the retina. A and B show light-induced GCaMP6 increases in fluorescence in three cells. The images in A and B were obtained immediately after and 1.35 s after the onset of light stimulation, respectively. Although cells 1, 2 and 3 were light-responsive, the better-focussed cell 1 was targeted for electrophysiological recordings. C) Current clamp traces showing the responses of cell 1 to current injections to -15 and -5 pA from a holding current of -35 pA. The steps to -5 pA evoked repetitive spiking. D) Current-clamped light responses versus intensity from cell 1. The intensity of the 480-nm light stimulus, expressed as photons/cm^2/s, is shown on the right. The bottom bar shows the timing of the light. The asterisks denote presumed spontaneous waves.

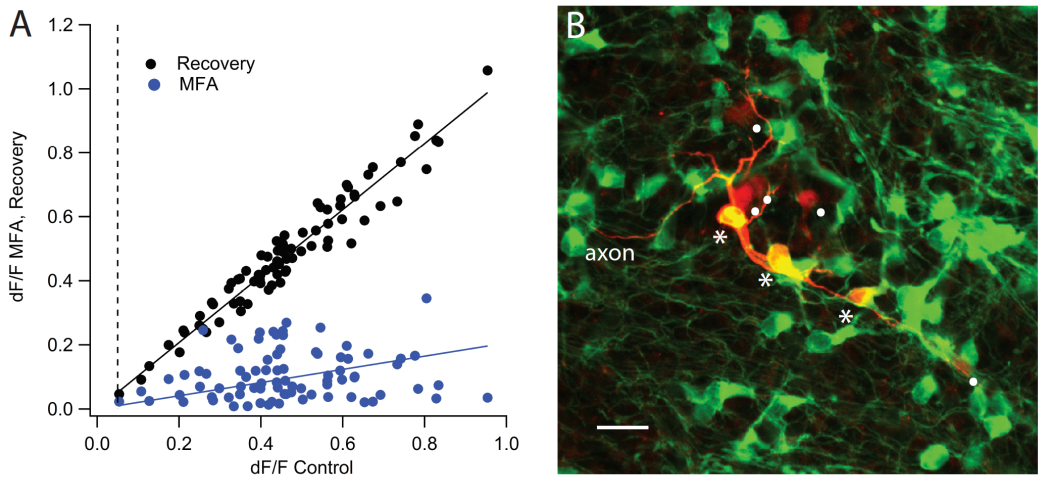

Figure 10

MFA, a gap junction-blocking drug, and intracellular neurobiotin injection reveal gap junction coupling between mRGCs in embryonic retinas.

A) Meclofenamic acid (50 mM) strongly and reversibly reduces light responses in E16.5 mRGCs. (Top panel) Light-evoked dF/F of 81 fluorescent cells in 2 retinas containing mRGCs expressing GCaMP6 (OPN4cre::Ai96). dF/F in 50 mM MFA (blue dots) and following washout (black dots) was plotted versus control dF/F. The data include 81 of 142 light-responsive cells in which the response after recovery was at least 80% and no more than 120% of the control value (note that 142 cells responded to light onset under control conditions with dF/F's > 0.05 but that in many of these cells the response failed to recover to at least 80% of the control value). The data were fitted with lines passing through the origin. The best fitting linear regression lines were y = 1.04 x and y= 0.21 x for recovery and MFA, respectively. The two-tailed P-value, obtained using the Wilcoxon Rank Test for paired data, was 8.3×10^{-25}, indicating that MFA highly significantly attenuates light-evoked dF/Fs. MFA reversibly attenuated light responses in essentially all the mRGCs.

B) Example of a neurobiotin injection (red) into an E18.5 mRGC. Three somas were neurobiotin- and EGFP-positive (green), indicative of tracer migration from one GCaMP6-expressing mRGC to at least two other mRGCs (stars). Five other somas (dots) were neurobiotin-positive (red) but lacked EGFP immunoreactivity, implying that mRGCs are coupled to non-melanopsin cells. The axon of the filled cell continued well beyond the picture to the left. The white scale bar indicates 20 μm.